NPS-MA-96-002

NAVAL POSTGRADUATE SCHOOL
Monterey, California

BUCKLING OF SHIP GRILLAGES

by

D.A. Danielson
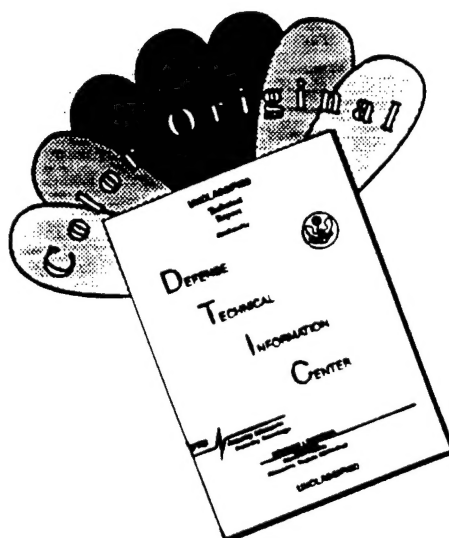D.P. Kihl

September 1996

Prepared for: Naval Postgraduate School
Monterey, CA 93943-5000

and

Naval Surface Warfare Center
Carderock Division
Washington, DC 20084-5000

19961104 056

DISCLAIMER NOTICE

THIS DOCUMENT IS BEST QUALITY AVAILABLE. THE COPY FURNISHED TO DTIC CONTAINED A SIGNIFICANT NUMBER OF COLOR PAGES WHICH DO NOT REPRODUCE LEGIBLY ON BLACK AND WHITE MICROFICHE.

NAVAL POSTGRADUATE SCHOOL
Monterey, California

Rear Admiral M.J. Evans
Superintendent

R. Elster
Provost

This report was prepared for and funded by the Naval Postgraduate School and the Naval Surface Warfare Center, Carderock Division, Washington, DC.

Reproduction of all or part of this report is authorized.
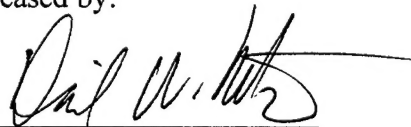
The report was prepared by:

_____
Donald Danielson
Professor
Department of Mathematics

Reviewed by:

_____
Richard Franke
Chairman
Department of Mathematics

Released by:

_____
David W. Netzer
Associate Provost and Dean of Research

REPORT DOCUMENTATION PAGE

1. AGENCY USE ONLY (Leave blank) September 1996	2. REPORT DATE	3. REPORT TYPE AND DATES COVERED Technical Report October, 1995 – September 1996

4. TITLE AND SUBTITLE

BUCKLING OF SHIP GRILLAGES

5. FUNDING NUMBERS

6. AUTHOR(S)

D. A. Danielson
D.P. Kihl

N00167-96-WR-60226

7. PERFORMING ORGANIZATION NAME(S) AND ADDRESS(ES)

Naval Postgraduate School
Code MA/Dd
Monterey, CA 93943

Naval Surface Warfare
Center
Code 653
Carderock Division
Bethesda, MD 20084-5000

8. PERFORMING ORGANIZATION REPORT NUMBER

NPS-MA-96-002

9. SPONSORING/MONITORING AGENCY NAME(S) AND ADDRESS(ES)

Naval Surface Warfare Center
Carderock Division
Washington, D.C. 20084-5000

Naval Postgraduate School
Monterey, CA 93943

10. SPONSORING/MONITORING AGENCY REPORT NUMBER

11. SUPPLEMENTARY NOTES

The views expressed in this report are those of the author and do not reflect the official policy or position of the Department of Defense or the US Government.

12a. DISTRIBUTION/AVAILABILITY STATEMENT

Approved for public release; distribution is unlimited.

12b. DISTRIBUTION CODE

13. ABSTRACT (Maximum 200 words)

The subject of this report is the mechanical behavior of stiffened plates, basic structural components of ships and submarines. The buckling loads of grillages subjected to axial compression with and without lateral pressure are calculated using a finite element based eigenvalue analysis. Insights are obtained into the ways in which the buckling loads and modes vary with various grillage dimensions.

14. SUBJECT TERMS

Ship Grillages, Plates, Buckling, Structures
Finite Elements

15. NUMBER OF PAGES
48

16. PRICE CODE

17. SECURITY CLASSIFICATION OF REPORT Unclassified	18. SECURITY CLASSIFICATION OF THIS PAGE	19. SECURITY CLASSIFICATION OF ABSTRACT	20. LIMITATION OF ABSTRACT Unclassified

BUCKLING OF SHIP GRILLAGES

D. A. Danielson
Code MA/Dd
Naval Postgraduate School
Monterey, CA 93943

D. P. Kihl
Code 653
Naval Surface Warfare Center, Carderock Division
Bethesda, MD 20084-5000

September, 1996

ABSTRACT

The subject of this report is the mechanical behavior of stiffened plates, basic structural components of ships and submarines. The buckling loads of grillages subjected to axial compression with and without lateral pressure are calculated using a finite element based eigenvalue analysis. Insights are obtained into the ways in which the buckling loads and modes vary with various grillage dimensions.

CONTENTS

INTRODUCTION

Stiffened plates are basic structural components of ships and submarines. These structures are designed with generous safety margins against overall collapse triggered by buckling. The object of mathematical modeling is to determine design criteria to inhibit buckling at any stress less than yield. In our earlier work (see References), we have reviewed the existing literature and developed new methods for predicting the buckling loads of simple plate-beam structures. In the present work, we calculate the axial buckling loads of grillages with the use of a well-known finite element code. The goal is to determine the effect on the buckling loads of varying various grillage parameters.

The grillage now modeled consists of 3 base plates with 4 longitudinal and 2 transverse stiffeners. The dimensions of this grillage are denoted in the report by

a1 = length between transverse stiffeners

a2 = length between transverse stiffener and grillage end

b1 = width between longitudinal stiffeners

b2 = width between outer longitudinal stiffener and grillage side = b1/3

t1 = thickness of inner base plate

t2 = thickness of outer base plates = t1 $\times \dfrac{4}{3}$

dw1 = depth of longitudinal webs

tw1 = thickness of longitudinal webs

df1 = depth of longitudinal flanges

tf1 = thickness of longitudinal flanges

dw2 = depth of transverse webs

tw2 = thickness of transverse webs

df2 = depth of transverse flanges

tf2 = thickness of transverse flange.

1

The material chosen for this study is isotropic steel with Young's modulus $E = 3 \times 10^7$ psi and Poisson's ratio $\nu = .3$. The imposed boundary conditions are:

(1) One end of the grillage has all 3 displacement components zero and all 3 rotation components zero.

(2) The other end of the grillage where the force is applied has axial displacement constant with the other 2 displacement components zero and all 3 rotation components zero.

(3) The ends of the transverse stiffeners have vertical displacement zero but the other 2 displacement components and all 3 rotation components are free.

(4) All other nodes on the plates edges are completely free.

Because of the boundary conditions and the fact that the thickness t2 of the outer base plates is chosen to be $\frac{4}{3}$ times the thickness t1 of the inner base plate, the buckling deflections of the outer bays are usually small compared to the buckling deflections of the central bay. Thus we calculate the buckling stress in the *central* bay, defined as the initial end force divided by the cross-sectional area of the central bay, even though actual buckled members may be elsewhere.

The finite element code used is MSC Nastran/Patran. The pre-processing and post-processing is done with Patran (versions 1.4 and 1.5). The buckling analysis (solution 105) is done with Nastran (version 68). The base plates, flanges, and webs are each modeled with Quad 4 plate elements. The mesh size is denoted in this report by

m1 = mesh length of all elements, mesh width of base plate elements

m2 = mesh width of web and flange elements.

That is, the base plating has square elements of size m1 × m1, while the webs and flanges have rectangular elements of size m1 × m2. Note that this is a full finite element model of the entire grillage and does not assume symmetry. We use linear geometry for the axial load only cases, nonlinear geometry for the pressure cases, and linear material properties for all

2

cases. All computations are performed on a Silicon Graphics Indy Workstation.

The first phase of our work is to compare the finite element model with experimental results on a small scale grillage under axial and pressure loading. The second phase is to vary the dimensions on a full scale model to assess changes in buckling stress and mode under axial load only.

EXPERIMENTALLY TESTED GRILLAGES

We first consider the grillages (Figure 1) tested in the USNA Ship Structures Laboratory testing rig (Figure 2). We choose the following values for the model parameters:

$a1 = 36''$

$a2 = 36''$

$b1 = 9''$

$t1 = \dfrac{3}{16}''$

$dw1 = 3''$

$tw1 = .114''$

$df1 = 1.844''$

$tf1 = .171''$

$dw2 = 9''$

$tw2 = .25''$

$df2 = 3''$

$tf2 = .25''$

$m1 = 1''$

$m2 = .5''.$

We find that the buckling load is not significantly changed by adopting smaller values for the mesh sizes m1 or m2.

The prebuckling stage is approximately one of uniform axial compression with little bending (Figure 3). The grillage buckles under a force of 470 kips. The buckling mode is a deformation involving primarily bending with little stretching (Figure 4). The inner base plate buckles into a square quilt of half-wavelength $9''$ (Figure 5). The webs (both transverse and longitudinal) also buckle with half-wavelength $9''$ (Figures 6-7). The flanges mainly just twist about their center line. We call this buckling mode TRIPPING to be consistent with

our earlier papers. *

We also ran nonlinear analyses (solution 106) for the cases of bottom pressure p = 0, p = 5 psi, or p = 20 psi. For the case p = 0, the plate only compresses in-plane and does not buckle. However, the buckles are clearly visible by the time the axial load reaches 475 kips for the p = 5 psi case and 450 kips for the p = 20 psi case. But since the buckling pattern develops gradually as the axial load increases, it is hard to pin down an exact "buckling" load. It is interesting that the middle plate develops only 3 half waves (instead of 4 as in the buckling analysis for p = 0). The magnitude of displacement for the p = 20 psi case is shown in Figure 8 with no axial load, and in Figure 9 with 550 kips axial load. If we increase the load much further than 500 - 550 kips, the displacements become large and the code will not give a solution (Figure 10).

A table comparing model results to experimentally measured collapse loads for 6 nominally identical grillages is given below:

p (psi)	Model (kips)	Experiments (kips)
0	470	326, 312, and 301
5	less than 475	316
10	not calculated	306
20	less than 450	296

---

*In our earlier work, we did not allow the stiffener cross-section to deform in its plane. This assumption led to a predicted buckling load which was much too high.

Note that both theory and experiments indicate that the presence of lateral pressure (on the plating side) tends to weaken the grillages. The disparity between the buckling loads of the perfect model and the experimental measurements is probably due to geometric imperfections, residual stress, differing boundary conditions, nonlinear material properties, etc. in the tested grillages.
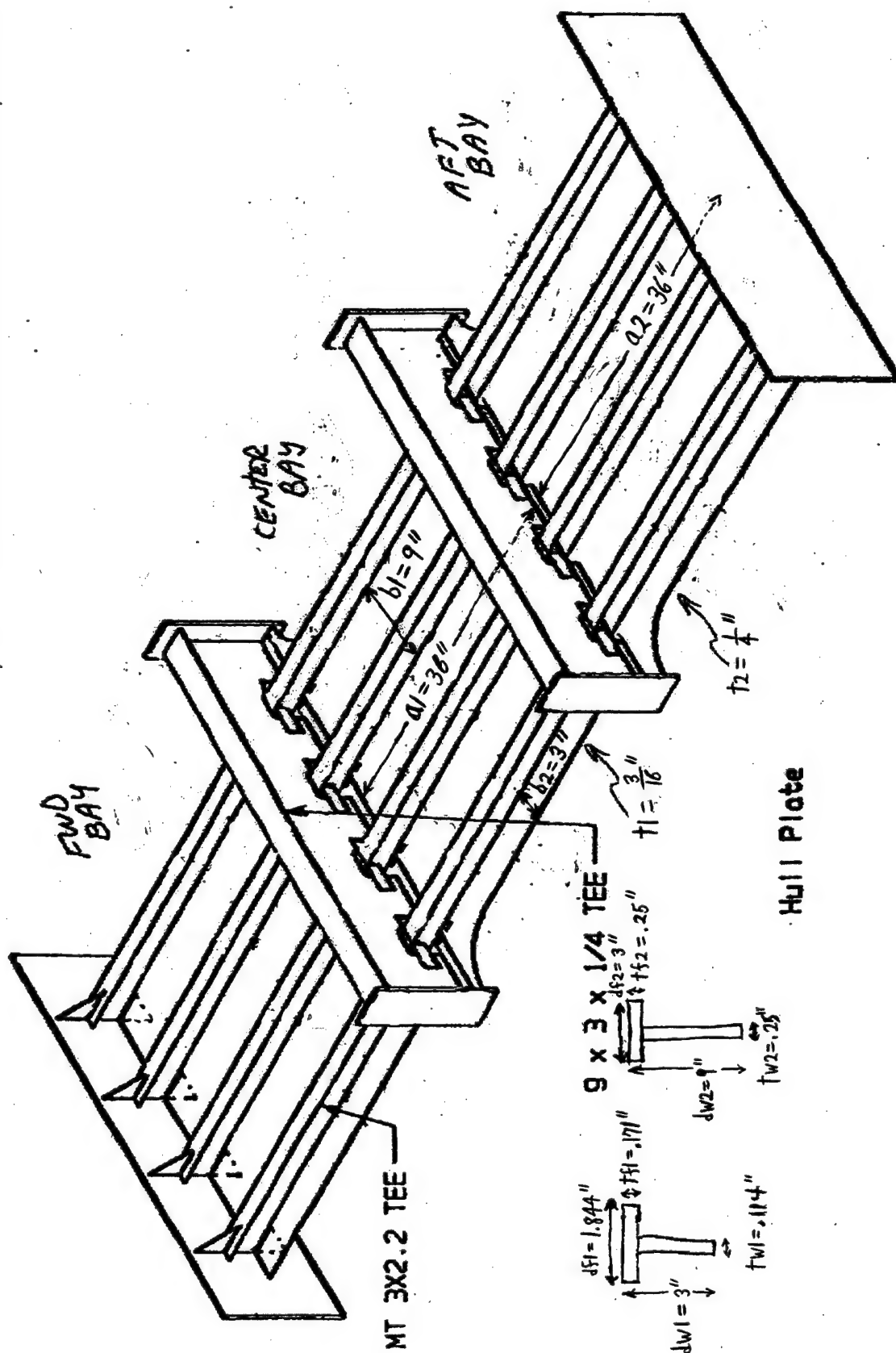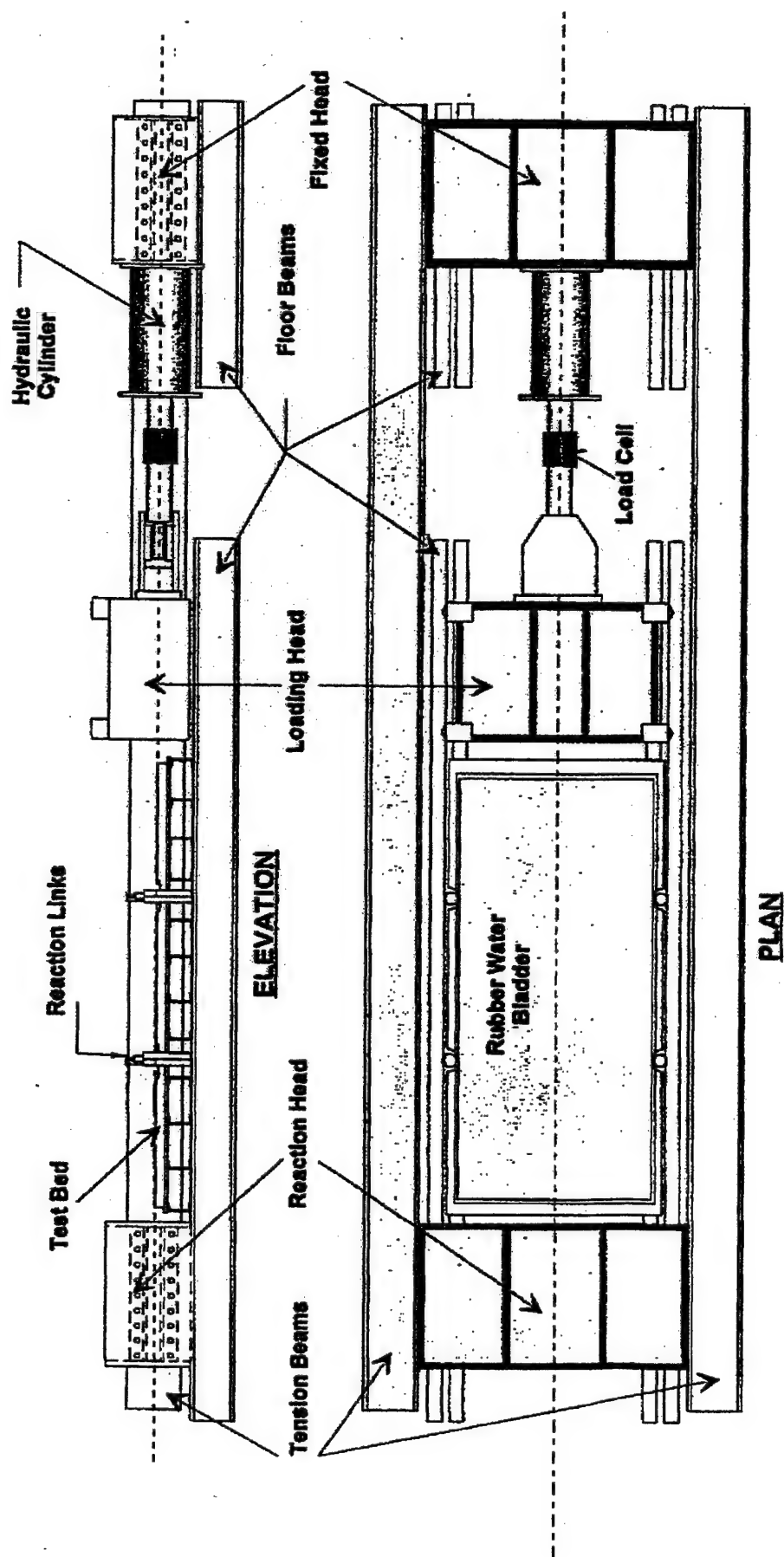
FWD BAY

CENTER BAY

AFT BAY

$b_1 = 9''$

$a_1 = 36''$

$a_2 = 36''$

$t_2 = \frac{1}{4}''$

$b_2 = 3''$

$t_1 = \frac{3}{16}''$

MT 3X2.2 TEE

9 x 3 x 1/4 TEE

$d_{f2} = 3''$

$t_{f2} = .25''$

$d_{w2} = 9''$

$t_{w2} = .25''$

$d_{f1} = 1.844''$

$t_{f1} = .171''$

$t_{w1} = .114''$

$d_{w1} = 3''$

Hull Plate

Figure 1

7

Hydraulic Cylinder

Fixed Head

Floor Beams

Load Cell

Loading Head

ELEVATION

Reaction Links

Rubber Water Bladder

Test Bed

Reaction Head

Tension Beams

PLAN

SCALE (in meters)

0.0   0.5   1.0

USNA Ship Structures Laboratory testing rig.

Figure 2

8

FRINGE PLOT LC=1.23 RES=2.1(VEC-MAG) MSC/PATRAN R-1.4 MSC/NASTRAN 29-Jan-96 11:55:35
DEFORMATION PLOT LC=1.23 RES=2.1 MSC/PATRAN R-1.4 MSC/NASTRAN 29-Jan-96 11:55:35

Prebuckling magnitude of displacements

.0000003540
.0000003310
.0000003070
.0000002830
.0000002600
.0000002360
.0000002130
.0000001890
.0000001650
.0000001420
.0000001180
.00000009400
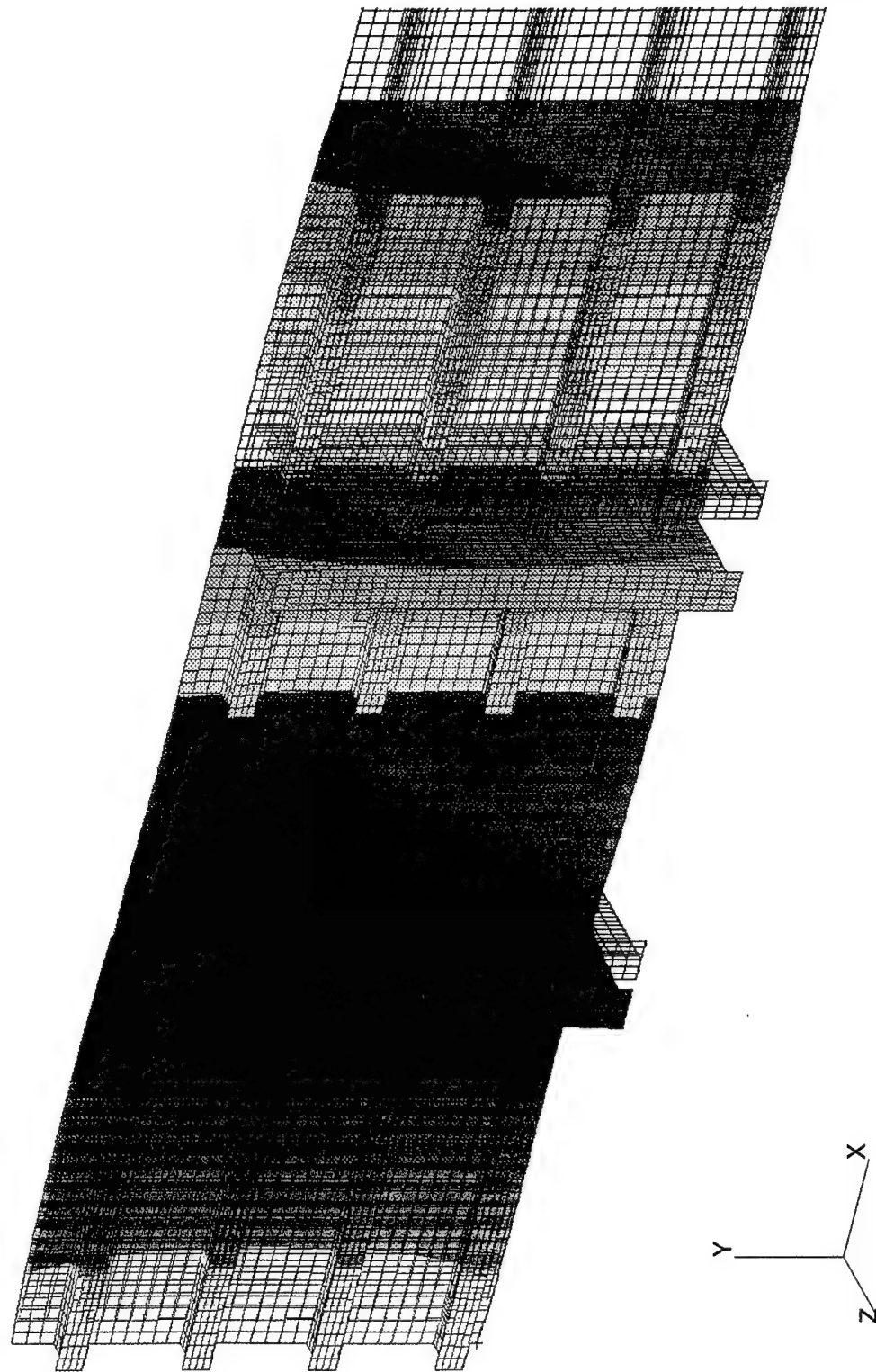.00000007100
.00000004700
.00000002400
.00000000000

Figure 3

FRINGE PLOT LC=2.24 RES=3.1(VEC-MAG) MSC/PATRAN R-1.4 MSC/NASTRAN 29-Jan-96 13:17:22
DEFORMATION PLOT LC=2.24 RES=3.1 MSC/PATRAN R-1.4 MSC/NASTRAN 29-Jan-96 13:17:22

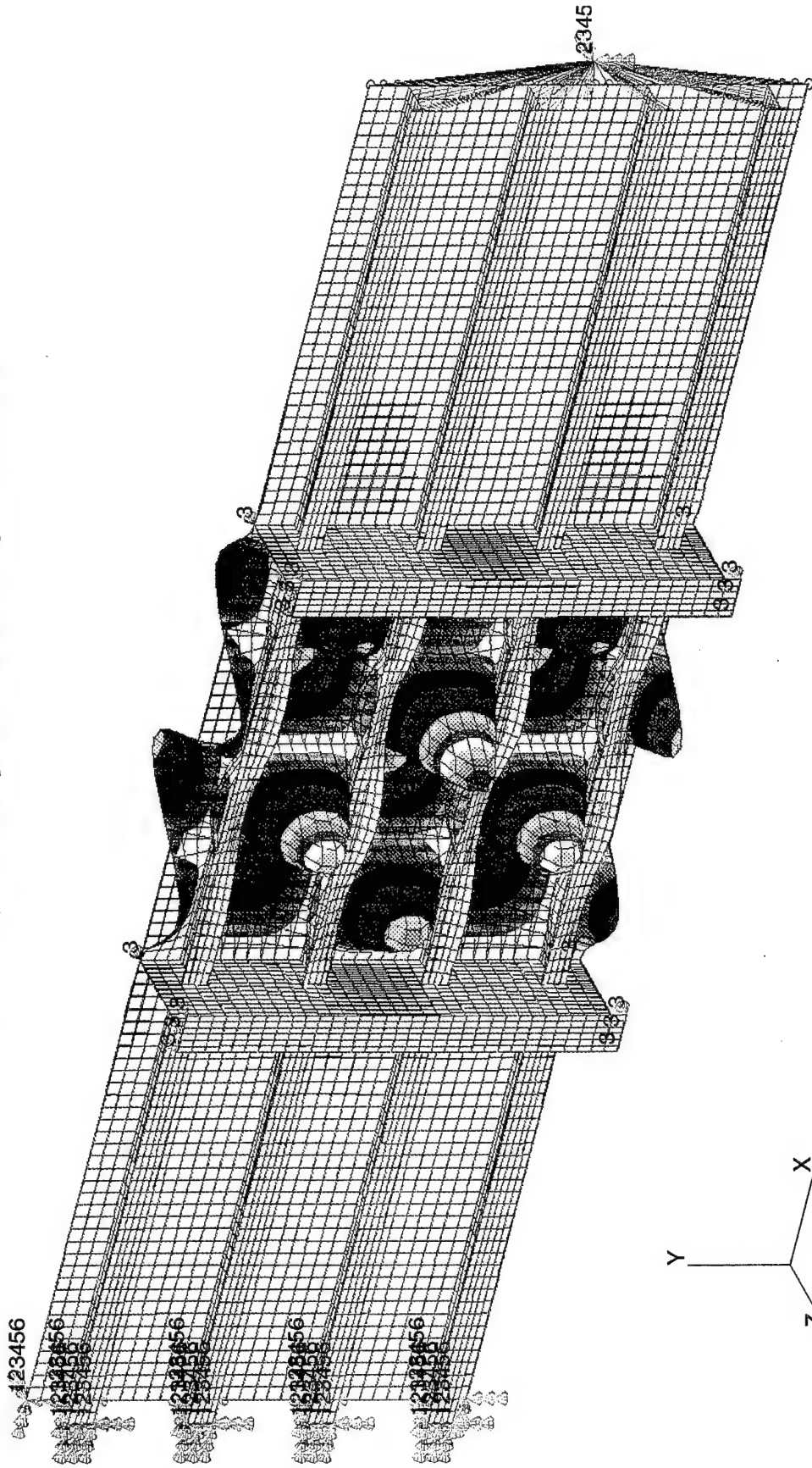470 kips - Magnitude of displacement

1.000
.9333
.8667
.8000
.7333
.6667
.6000
.5333
.4667
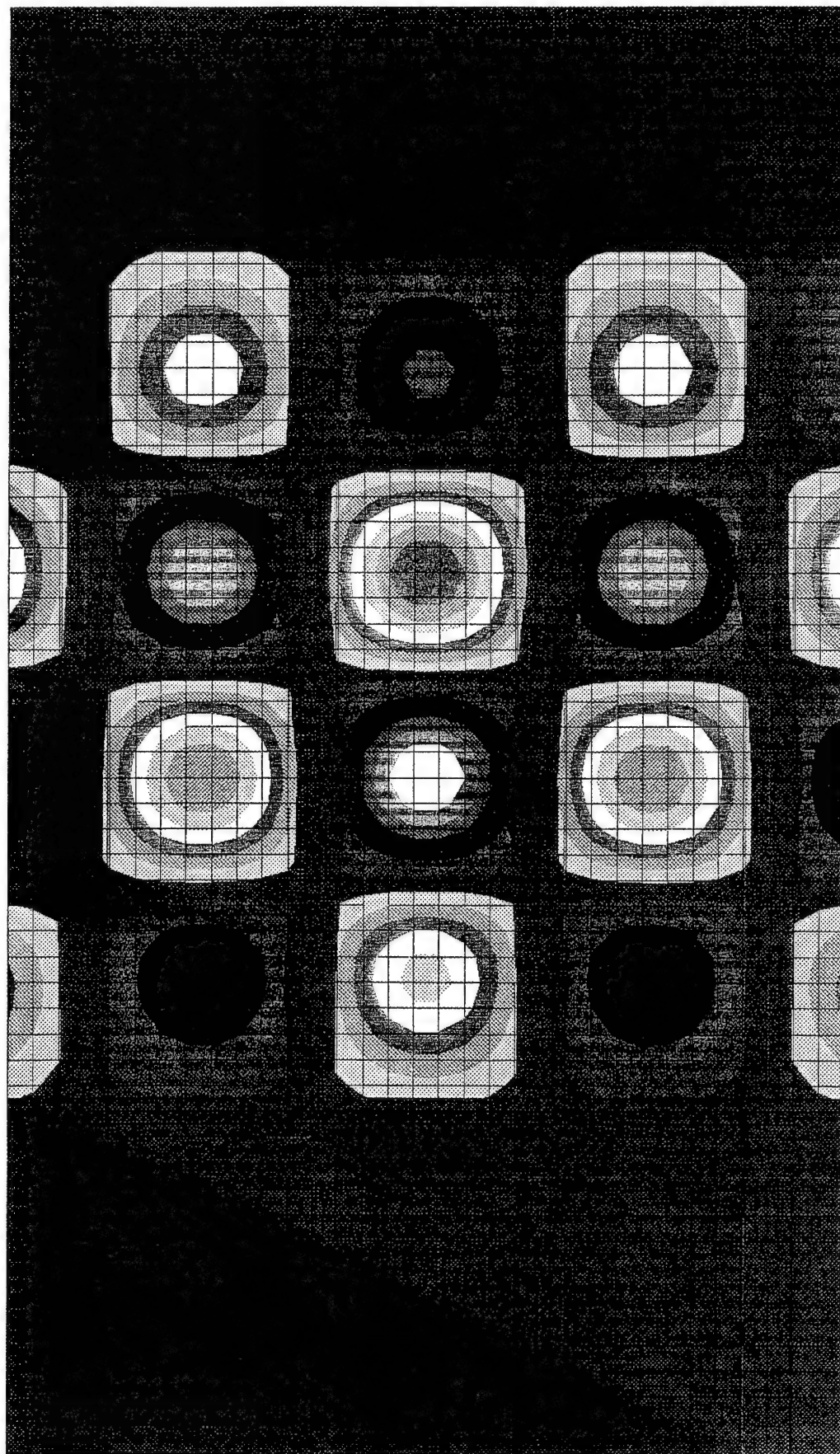.4000
.3333
.2667
.2000
.1333
.06667
.00000004500

Figure 4

FRINGE PLOT LC=2.24 RES=3.1(Z-COMP) MSC/PATRAN R-1.4 MSC/NASTRAN 29-Jan-96 13:31:39
DEFORMATION PLOT LC=2.24 RES=3.1 MSC/PATRAN R-1.4 MSC/NASTRAN 29-Jan-96 13:31:39

470 kips - z displacement

1.000
.8667
.7333
.6000
.4667
.3333
.2000
.06667
-.06667
-.2000
-.3333
-.4667
-.6000
-.7333
-.8667
-1.000

Figure 5

11

.01497
.01290
.01083
.008754
.006682
.004610
.002538
.0004656
-.001607
-.003679
-.005751
-.007823
-.009895
-.01197
-.01404
-.01611

470 kips - x displacement

T_ LC=2.24 RES=3.1(X-COMP) MSC/PATRAN R-1.4 MSC/NASTRAN 29-Jan-96 13:40:05
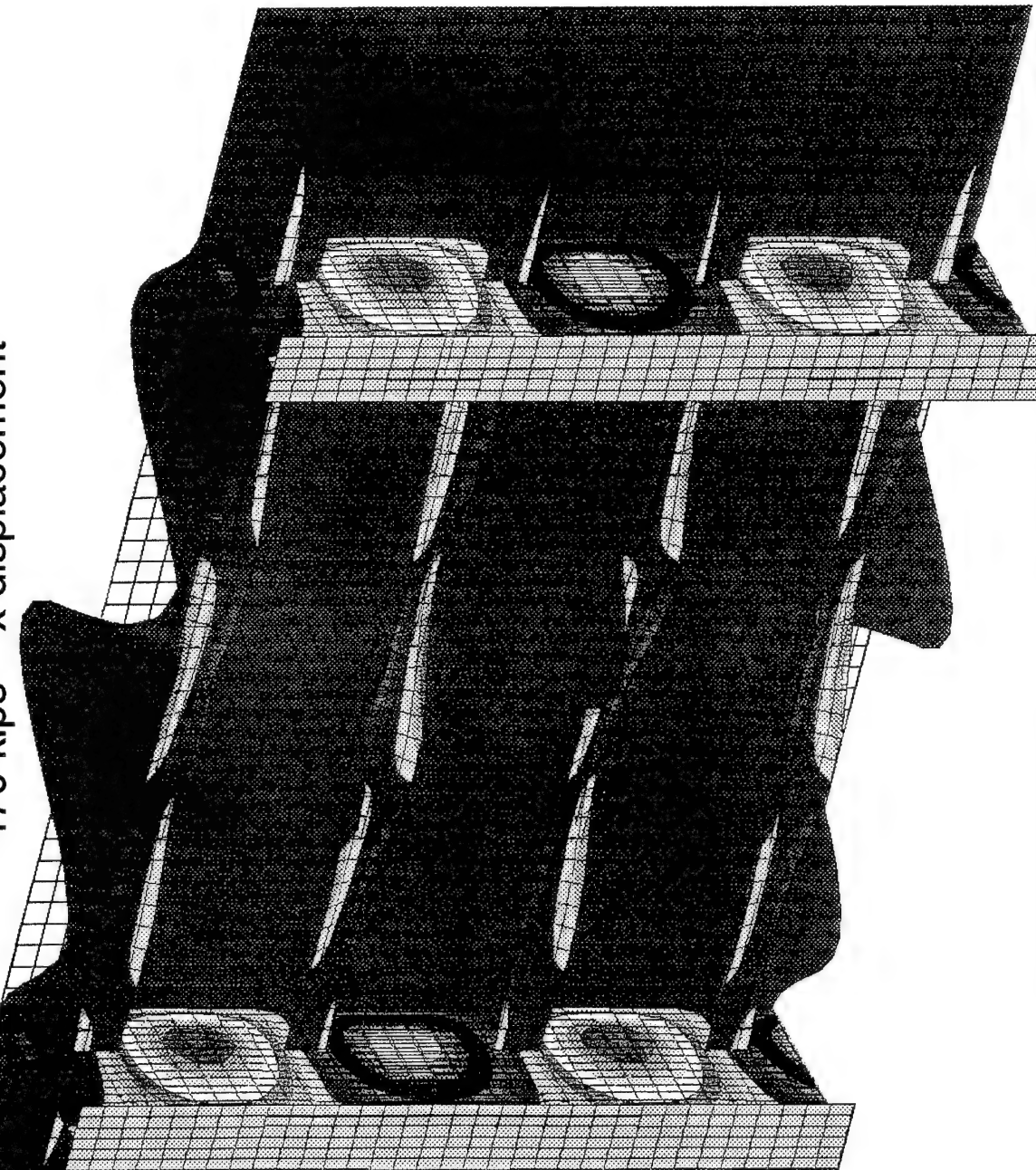6=2.24 RES=3.1 MSC/PATRAN R-1.4 MSC/NASTRAN 29-Jan-96 13:40:05

Figure 6

12

470 kips - y displacement

T LC=2.24 RES=3.1(Y-COMP) MSC/PATRAN R-1.4 MSC/NASTRAN 29-Jan-96 13:46:30
2.24 RES=3.1 MSC/PATRAN R-1.4 MSC/NASTRAN 29-Jan-96 13:46:30

.1522
.1319
.1116
.09130
.07101
.05072
.03043
.01014
-.01014
-.03043
-.05072
-.07101
-.09130
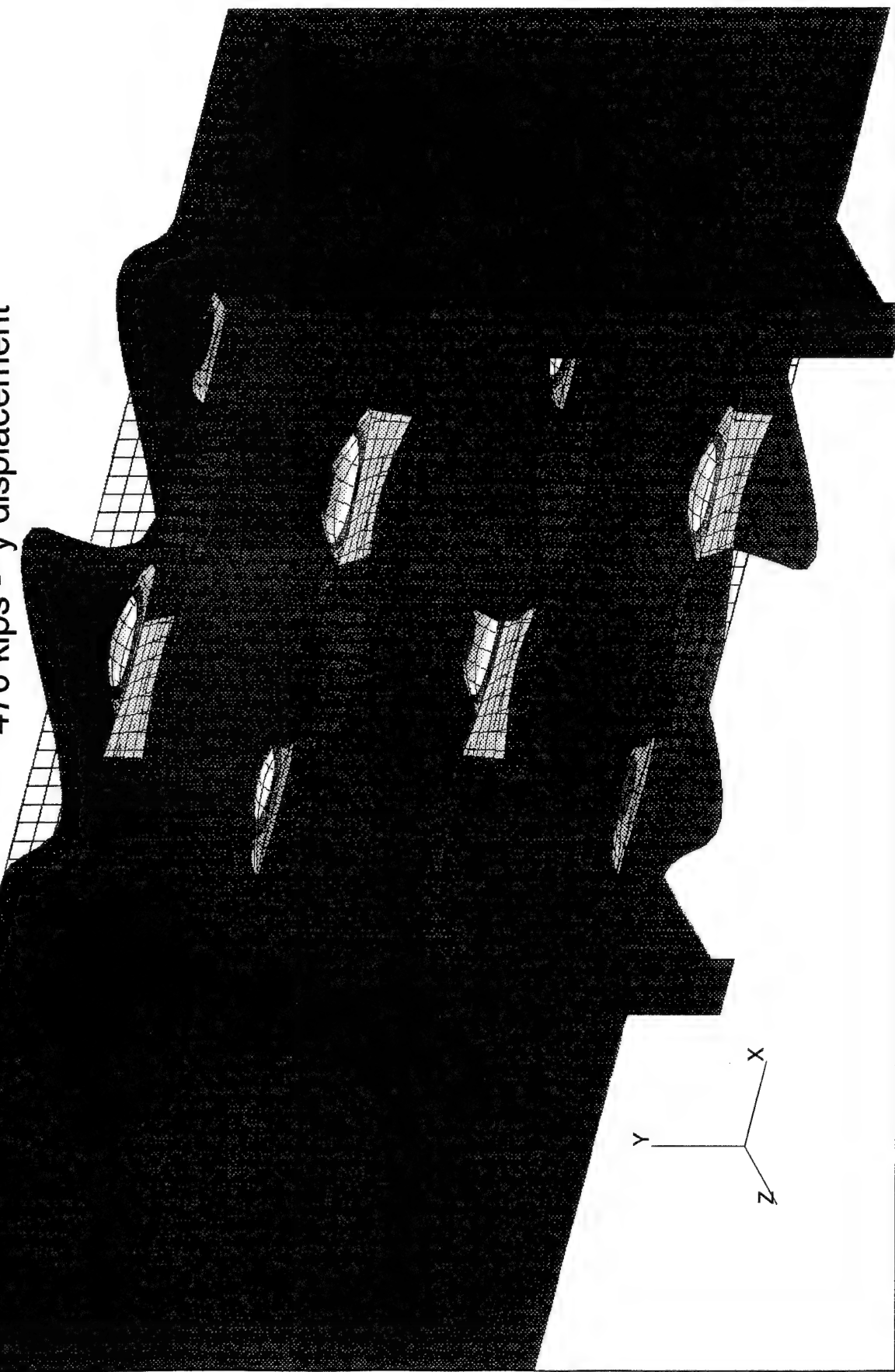-.1116
-.1319
-.1522

Figure 7

13

FRINGE PLOT LC=4.79 RES=2.1(VEC-MAG) MSC/PATRAN R-1.4 MSC/NASTRAN 12-Feb-96 10:18:49
DEFORMATION PLOT LC=4.79 RES=2.1 MSC/PATRAN R-1.4 MSC/NASTRAN 12-Feb-96 10:18:49

.04989
.04657
.04324
.03991
.03659
.03326
.02994
.02661
.02328
.01996
.01663
.01330
.009979
.006652
.003326
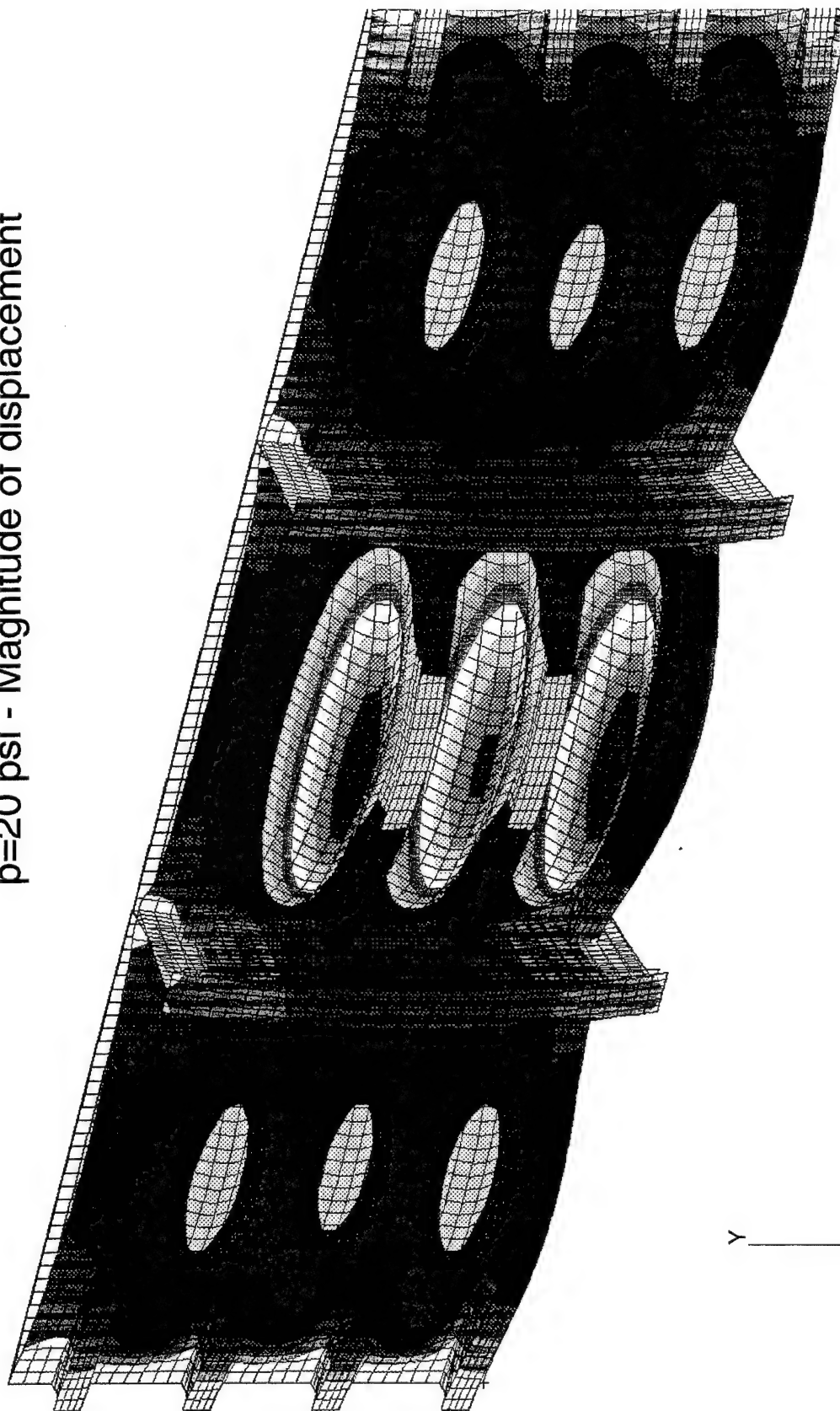.000000007000

p=20 psi - Magnitude of displacement

Figure 8

14

FRINGE PLOT LC=3.90 RES=2.1(VEC-MAG) MSC/PATRAN R-1.4 MSC/NASTRAN 12-Feb-96 10:37:53
DEFORMATION PLOT LC=3.90 RES=2.1 MSC/PATRAN R-1.4 MSC/NASTRAN 12-Feb-96 10:37:53

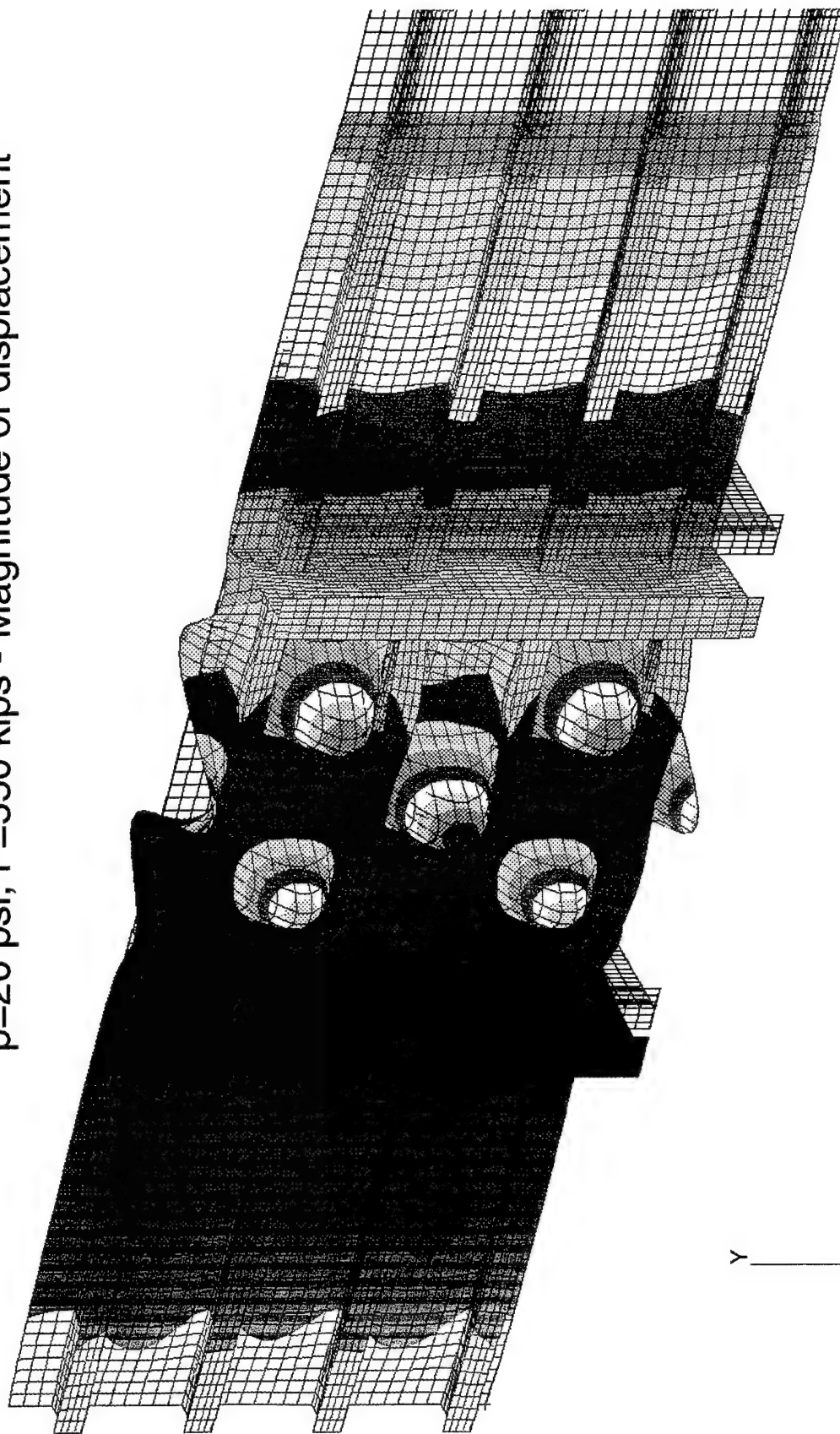p=20 psi, F=550 kips - Magnitude of displacement

.2220
.2072
.1924
.1776
.1628
.1480
.1332
.1184
.1036
.08882
.07401
.05921
.04441
.02961
.01480
-.000000003900

Figure 9

15

Center z-displacement

- ▪ p=5 psi
- ● p=20 psi

inches

.180
.150
.120
.0900
.0600
.0300
0.

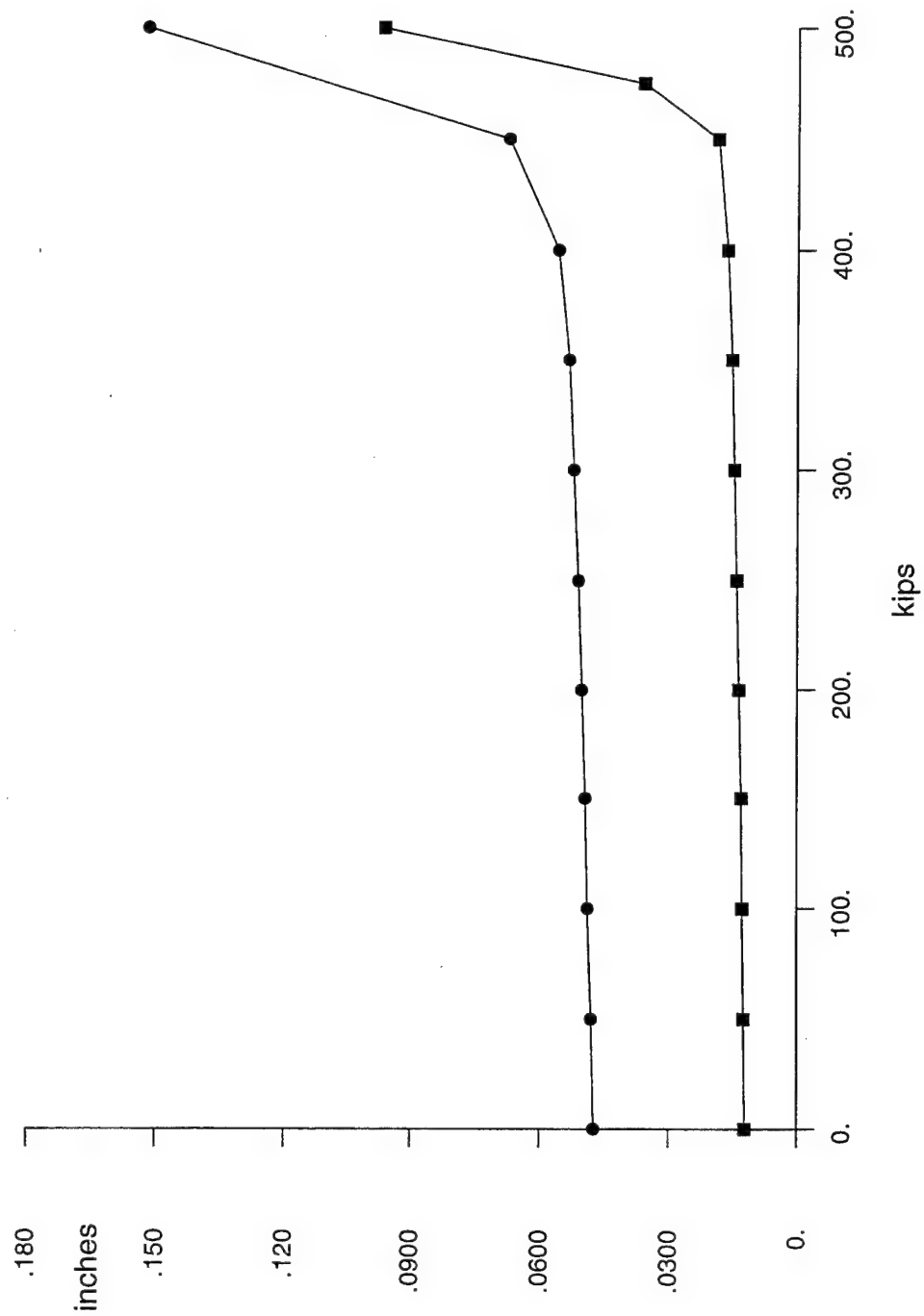0.   100.   200.   300.   400.   500.

kips

Figure 10

16

GRILLAGES OF VARIOUS DIMENSIONS

Generic model

We define the generic model as a grillage with the following parameter values:

$a1 = 96''$

$a2 = 48''$

$b1 = 24''$

$t1 = \dfrac{9}{16}''$

$dw1 = 6''$

$tw1 = .2''$

$df1 = 4''$

$tf1 = .225''$

$dw2 = 12''$

$tw2 = .2''$

$df2 = 4''$

$tf2 = .225''$

$m1 = 2''$

$m2 = 1''.$

The buckling stress in the central bay of the generic model is 66.2 ksi. The buckling mode is TRIPPING of the central bay (Figure 11). The half-wavelength of the buckles is 24″.

Note that the outer bays of the generic model are made half as long as the inner bay, to reduce the size of the finite element model. The buckling load of the full scale model differs from that of the generic model by an insignificant amount.

For the remainder of the report, we consider various grillages with only one dimension different from those of the generic model.

Variation of a1, length between transverse stiffeners

We consider 6 grillages having differing values of a1. All of the other parameters are the same as for the generic grillage, except for the case a1 = 144″ we choose the mesh length m1 = 4″ to make the program size smaller. The buckling stress decreases monotonically with a1 (Figure 12). The buckling mode is TRIPPING in all cases. For the 5 cases with a1 a multiple of 24″, the half-wavelength of the buckles is 24″. For the case a1 = 60″, the half-wavelength is 30″ (Figure 13).

Variation of b1, width between longitudinal stiffeners

We consider 4 grillages having b1 differing multiples of 12″. The buckling stress decreases monotonically with b1 (Figure 14). The buckling stress is somewhat larger than the classical buckling stress of a square simply-supported plate (Figure 15):

$$\frac{E\pi^2(t1)^2}{3(1-\nu^2)(b1)^2}$$

The buckling mode is TRIPPING (similar to Figure 11) and the half-wavelengths of the buckles is b1.

Variation of t1, thickness of inner base plate

We consider 5 grillages having differing values of t1. The buckling stress reaches a maximum value for an optimal t1 (Figures 16 - 17). For the 3 lowest cases, the buckling mode is TRIPPING, with the half-wavelengths being $19.2''$ for the case $t1 = \frac{3}{16}''$ and $24''$ for the cases $t1 = \frac{3}{8}''$ and $t1 = \frac{9}{16}''$ For the cases $t1 = \frac{3}{4}''$ and $t1 = \frac{15}{16}''$ the buckling mode is GLOBAL. The entire central bay buckles in (Figure 18), while the stiffeners deflect inwards and laterally (Figure 19).

Variation of dw1, depth of longitudinal webs

We consider 7 grillages having differing values of dw1. The buckling stress reaches a maximum value for an optimal dw1 (Figure 20). For the cases $dw1 = 3''$ and $dw1 = 4''$, the buckling mode is GLOBAL (Figure 21). For the cases $dw1 = 5''$, $dw1 = 6''$, and $dw1 = 9''$, the buckling mode is TRIPPING with half-wavelength of $24''$. For the cases $dw1 = 10''$ and $dw1 = 11''$, the buckling mode is LOCAL (Figure 22). The web and flange of a middle stiffener of the central bay buckle with a half-wavelength dw1. We find that the critical load for the local buckling case is not significantly changed by adopting smaller values for the web and flange mesh element width m2.

Variation of tw1, thickness of longitudinal webs

We consider 7 grillages having differing values of tw1. The buckling stress increases monotonically with tw1 (Figure 23). For the case $tw1 = .05''$, the web of a middle stiffener of the forward bay buckles LOCALLY, and for the case $tw1 = .1''$, the web of a middle stiffener of the central bay buckles LOCALLY (Figure 24). For the cases $tw1 = .15''$, $.2''$, $.3''$, and $.7''$ the buckling mode is TRIPPING with half-wavelength $24''$ (Figure 25). For the case $tw1 = 1''$, the buckling mode is TRIPPING with half-wavelength $19.2''$.

Variation of df1, depth of longitudinal flanges

We consider 4 grillages having differing values of df1. For the cases df1 = 2″, 4″, and 6″, the buckling mode is TRIPPING and the buckling stress varies little (Figure 26). For the case df1 = 0 (no flange), the web of a middle stiffener of the central bay buckles LOCALLY (Figure 27).

Variation of tf1, thickness of longitudinal flanges

We consider 4 grillages having different values of tf1. For the cases tf1 = .225″, .5″, and 1″, the buckling mode is TRIPPING and the buckling stress varies little (Figure 28). For the case tf1 =.1″, the flange of a middle stiffener of the central bay buckles LOCALLY (Figure 29).

Variation of dw2, depth of transverse webs

We consider 3 grillages having differing values of dw2. For all 3 cases dw2 = 4″, 12″, and 16″, the buckling mode is TRIPPING and the buckling stress varies little (Figure 30).

Variation of tw2, thickness of transverse webs

We consider 3 grillages having differing values of tw2. For the cases tw2 = .15″ and .2″, the buckling mode is TRIPPING and the buckling stress varies little (Figure 31). For the case tw2 = .1″, a web buckles LOCALLY under a *tensile* force (Figure 32). Compression in the web arises from Poisson ratio effects.

Variation of df2, depth of transverse flanges

We consider 2 grillages having differing values of df2. For both cases df2 = 0 (no flange) and df2 =4″, the buckling mode is TRIPPING and the buckling stress varies little (Figure 33). Note that eliminating the transverse flange would not reduce the buckling strength of the grillage under axial compression.

Variation of tf2, thickness of transverse flanges

We consider 2 grillages having differing values of tf2. For both cases tf2 $= .1''$ and tf2 $=.225''$, the buckling mode is TRIPPING and the buckling stress varies little (Figure 34).

Summary

Through study of all these different results, we can gain insights into the ways in which the buckling loads and modes vary with the various dimensions.

The buckling stress decreases less with length a1 than with width b1 between stiffeners. The buckling stress is larger for an optimal value of plating thickness t1 and depth dw1 of longitudinal webs. The buckling stress increases with thickness tw1 of longitudinal webs. The buckling stress is not much affected by increases in the dimension df1 and tf1 of the longitudinal flanges, dimensions dw2 and tw2 of transverse webs, or dimensions df2 and tf2 of transverse flanges. However, the buckling stress is smaller for too small values of thickness tw1 of longitudinal webs, depth df1 and thickness tf1 of longitudinal flanges, and thickness tw2 of transverse webs.

We have found three distinct failure modes which we have named TRIPPING, GLOBAL, and LOCAL. For the majority of our cases, the failure mode is TRIPPING with the inner base plate buckling into a square quilt, which forces the webs to buckle into a rectangular quilt with the same wavelength, while the flanges twist (Figure 11). However, if a square pattern cannot fit into the base plate (Figure 13), or if the relative strength of the stiffeners is much greater than the base plate (Figure 25), the inner base plate may buckle into a non-square quilt, and the flanges may also undergo lateral deformation. If the relative strength of the inner base plate is much greater than the stiffeners, the failure mode may be GLOBAL with the entire central bay buckling in (Figures 18-19 and 21). If the relative strength of a stiffener is too small, it may collapse LOCALLY before any of the other components buckle (Figures 22, 24, 27, 29, and 32).
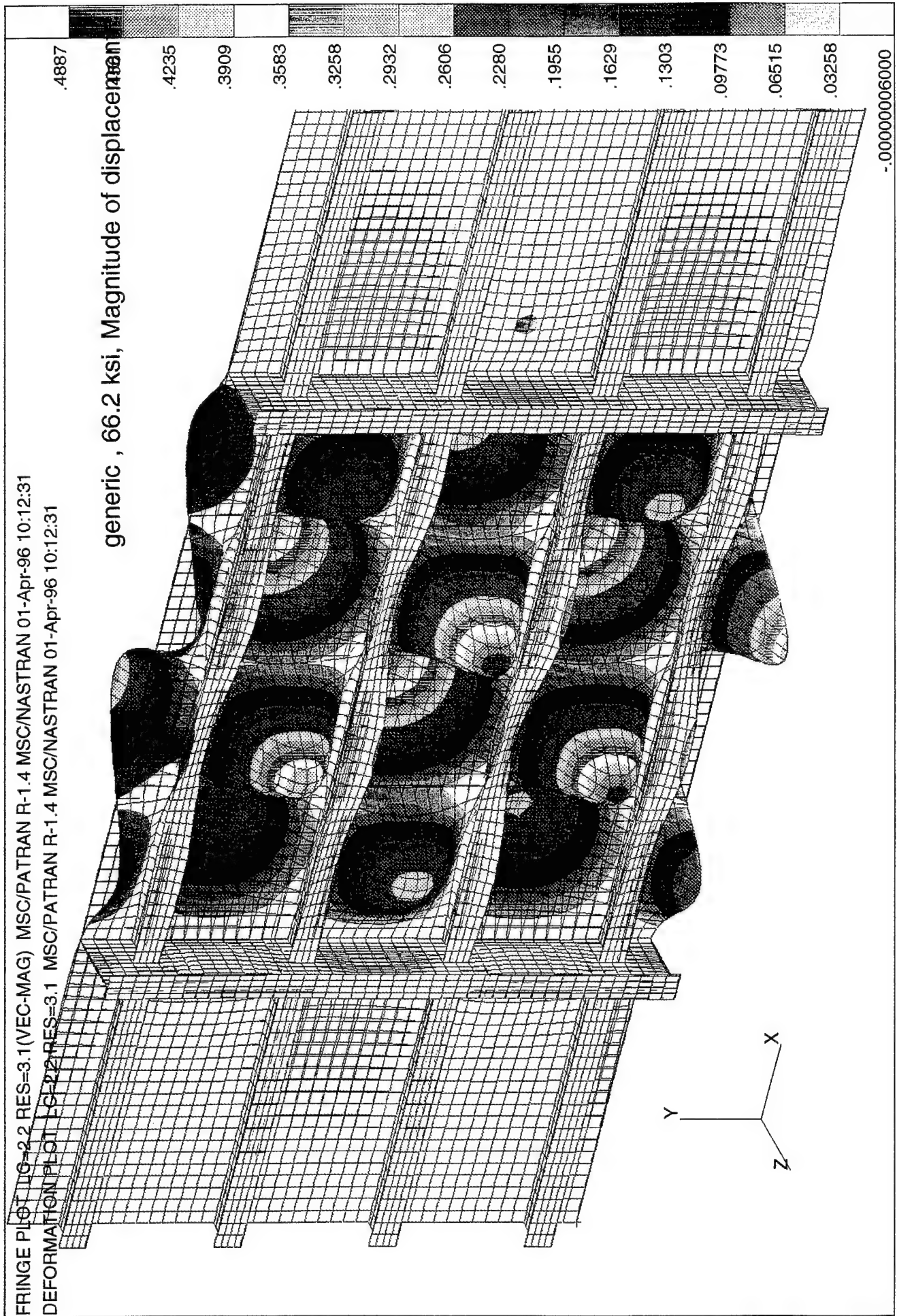
FRINGE PLOT: LG=2.2 RES=3.1(VEC-MAG) MSC/PATRAN R-1.4 MSC/NASTRAN 01-Apr-96 10:12:31
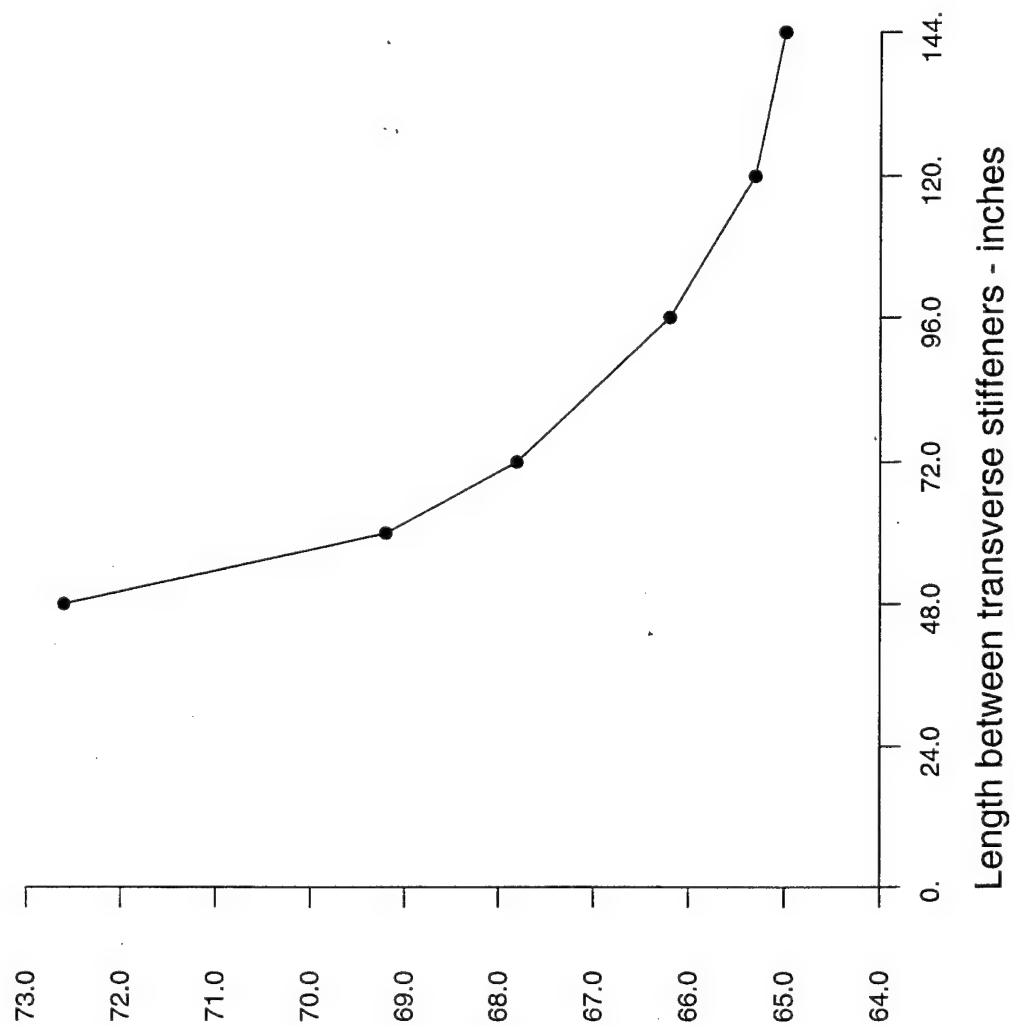DEFORMATION PLOT: LG=2.2 RES=3.1 MSC/PATRAN R-1.4 MSC/NASTRAN 01-Apr-96 10:12:31

generic , 66.2 ksi, Magnitude of displacement

.4887

.4235

.3909

.3583

.3258

.2932

.2606

.2280
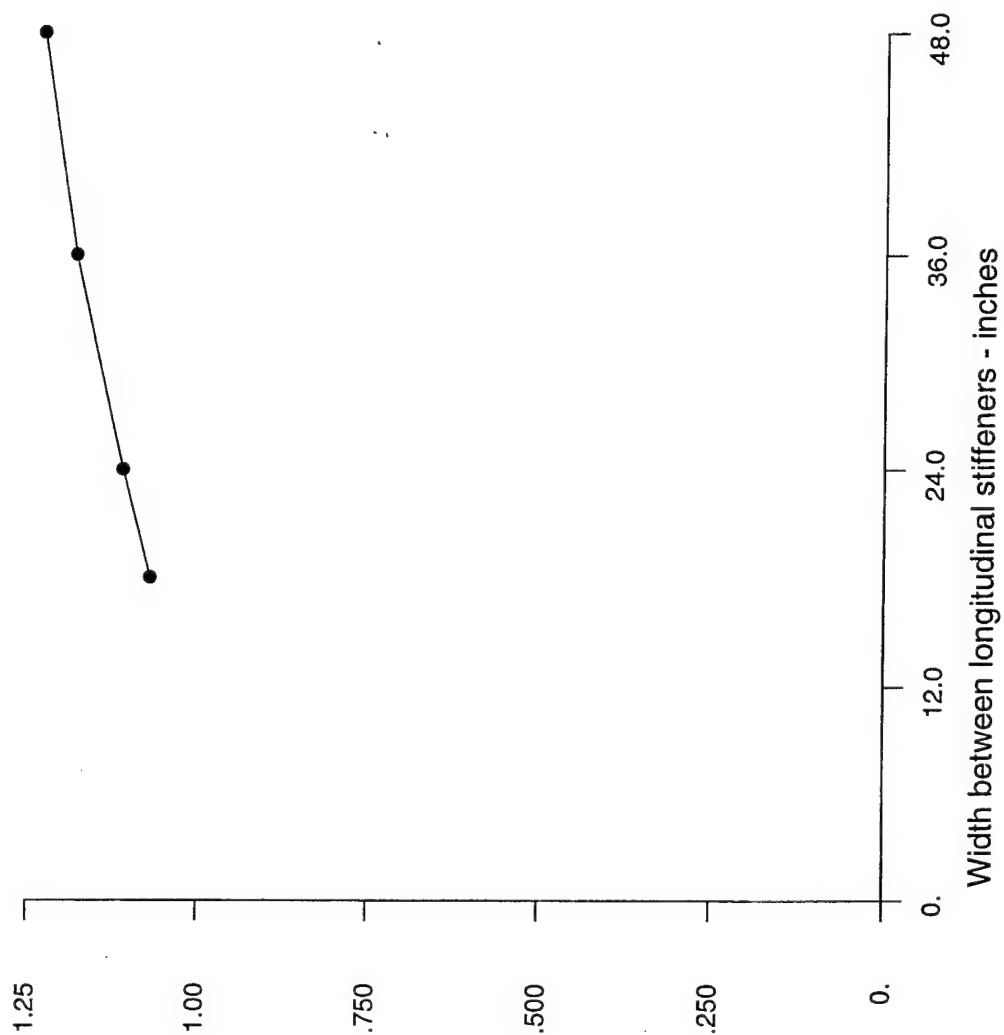
.1955

.1629

.1303

.09773

.06515

.03258

-.0000006000

Figure 11

22

Figure 12

FRINGE PLOT LC=2.2 RES=3.1(VEC-MAG) MSC/PATRAN R-1.4 MSC/NASTRAN 08-Mar-96 15:00:11
DEFORMATION123456 LC=2.2 RES=3.1 MSC/PATRAN R-1.4 MSC/NASTRAN 08-Mar-96 15:00:11

a1=60" , 69.2 ksi - Magnitude of displacement

.7189

.6709

.6230

.5751

.5272

.4792

.4313

.3834

.3355

.2875

.2396

.1917

.1438

.09585

.04792

-.00000005200

Figure 13

24

Buckling stress in central bay - ksi

Width between longitudinal stiffeners - inches

Figure 14

Figure 15

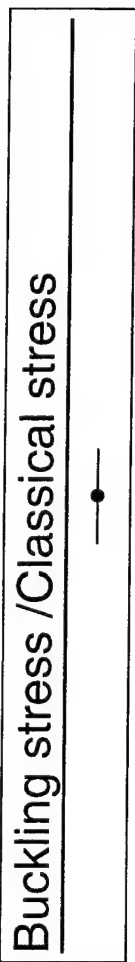Buckling stress /Classical stress

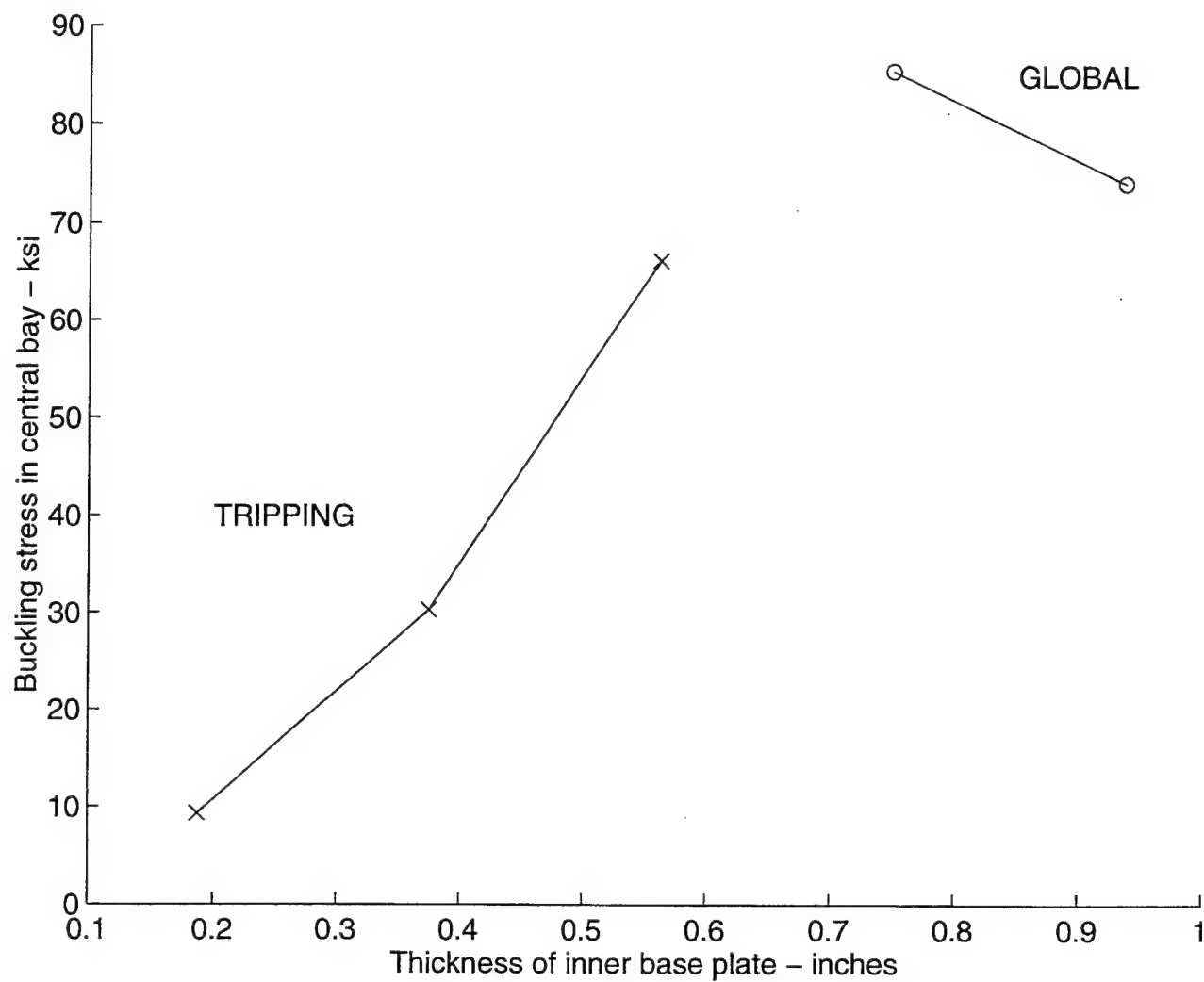Width between longitudinal stiffeners - inches
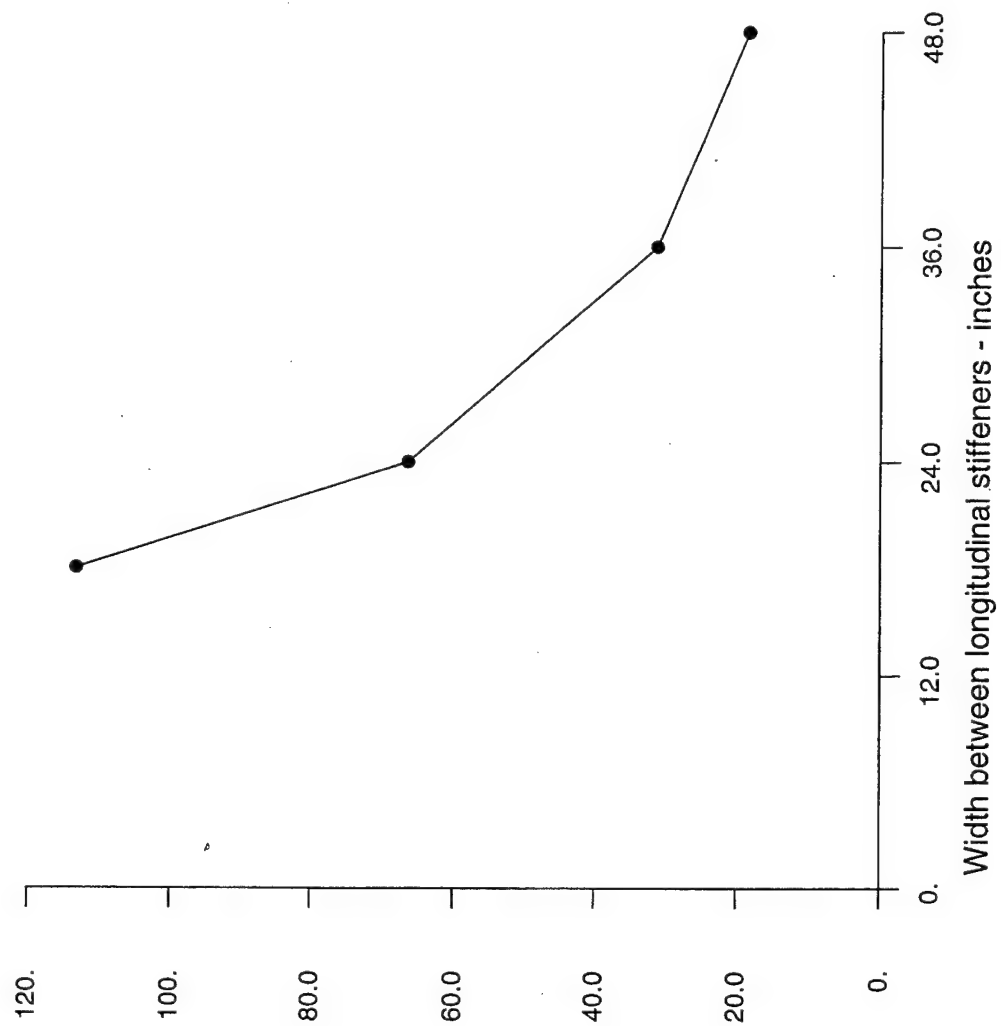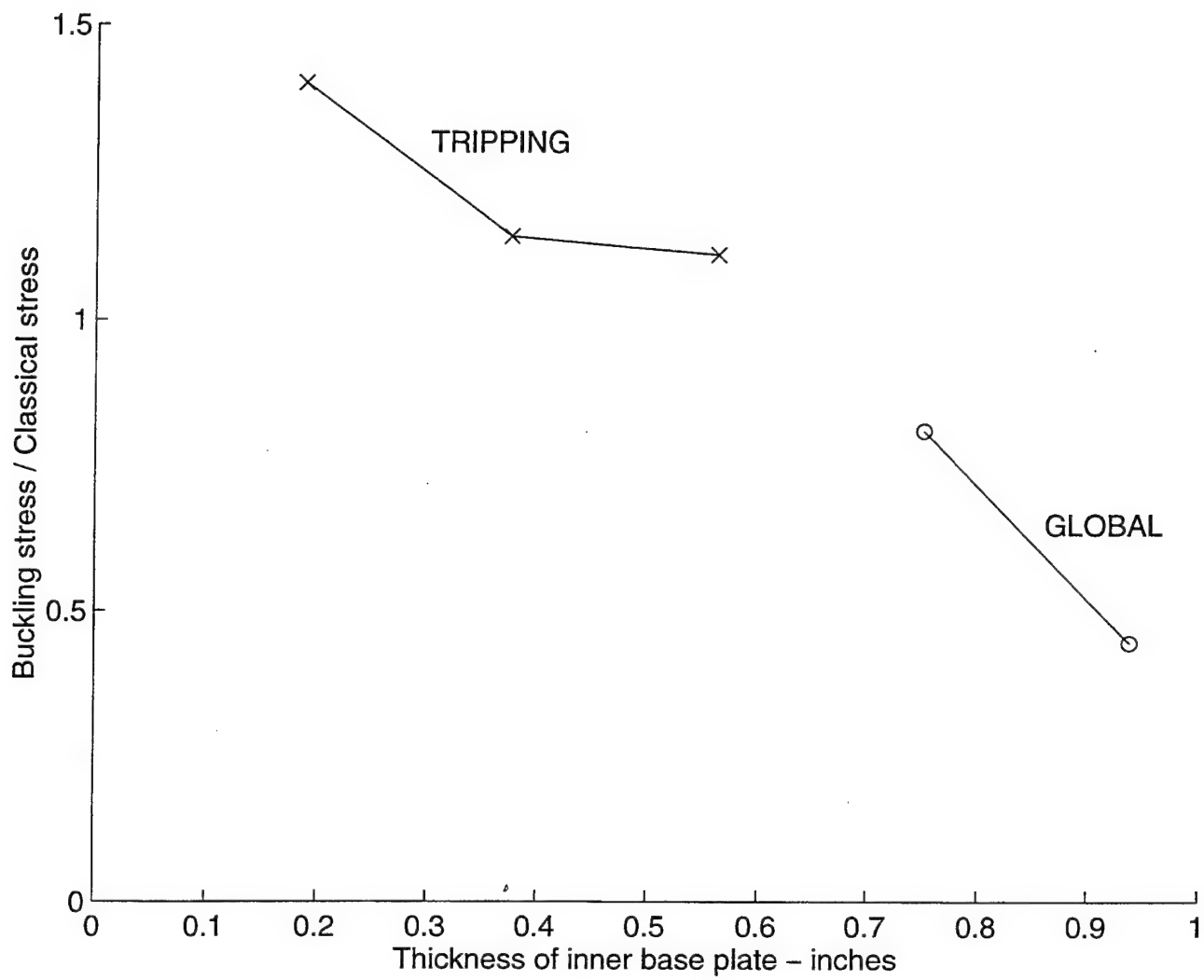
Figure 16

Figure 17

FRINGE PLOT LC=2.2 RES=3.1(Z-COMP) MSC/PATRAN R-1.4 MSC/NASTRAN 18-Mar-96 13:09:09
DEFORMATION PLOT LC=2.2 RES=3.1 MSC/PATRAN R-1.4 MSC/NASTRAN 18-Mar-96 13:09:09

t1=.9375" , 74.1 ksi, z-displacement

.009002
.002885
-.003233
-.009350
-.01547
-.02158
-.02770
-.03382
-.03994
-.04605
-.05217
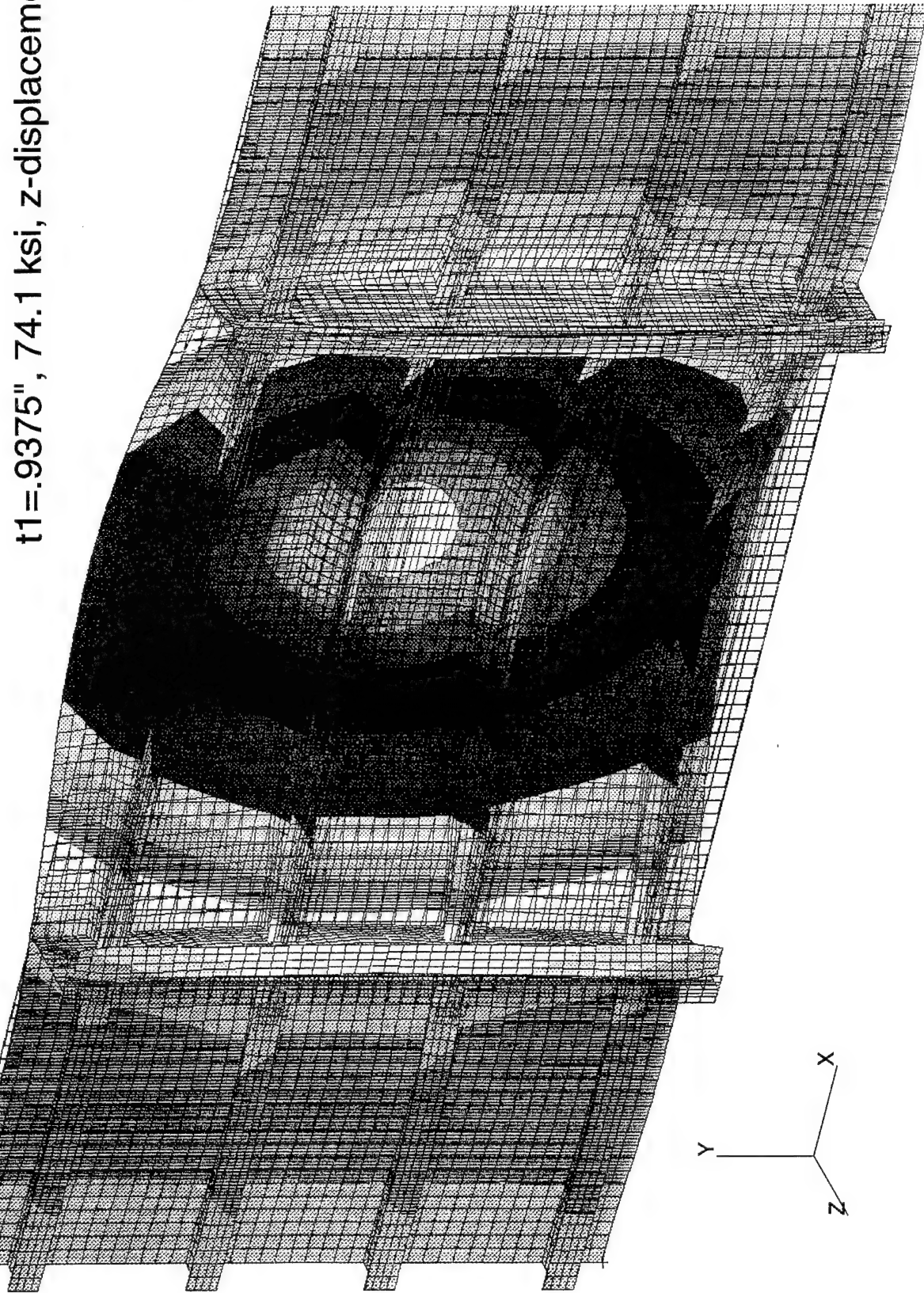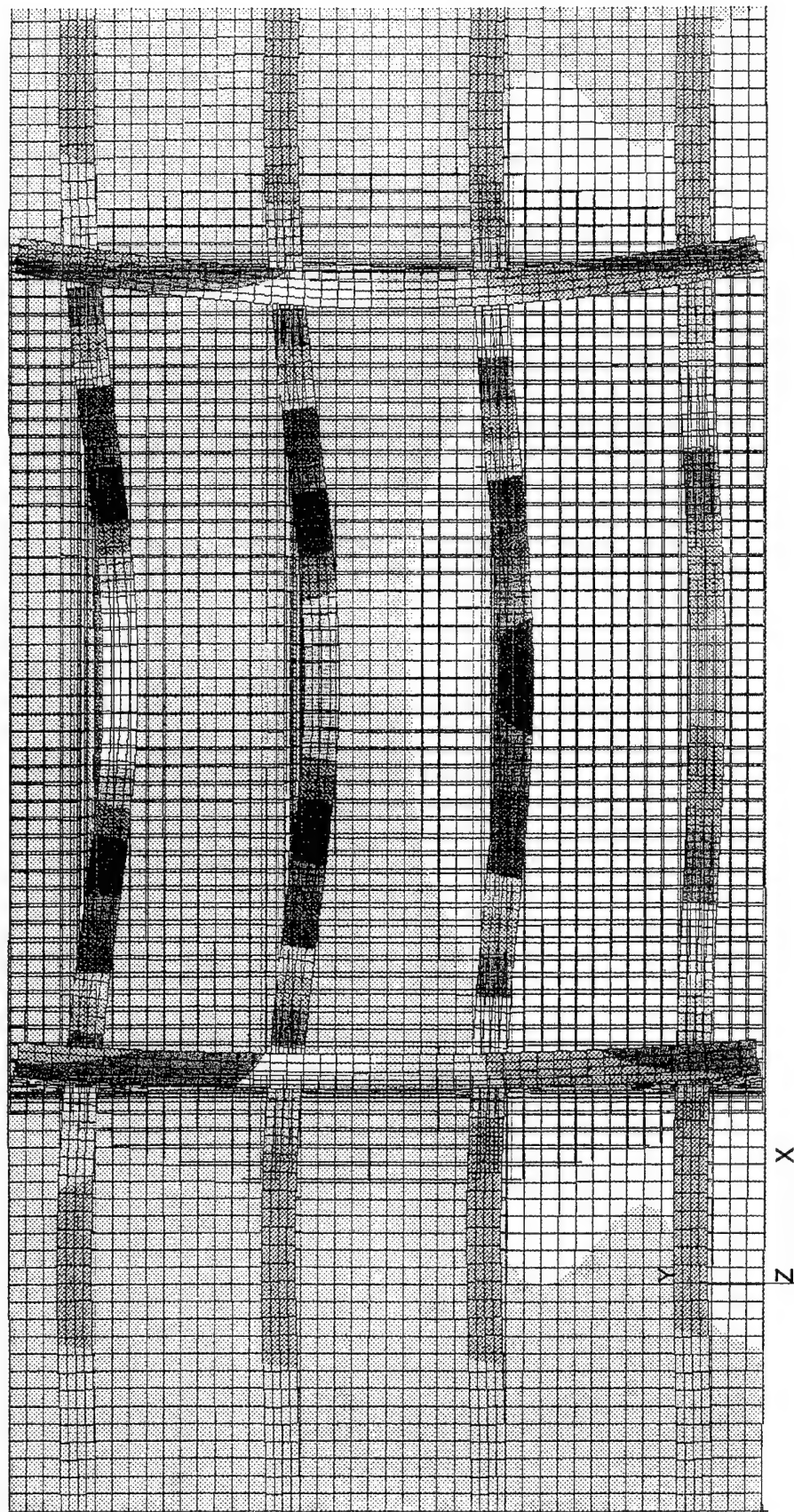-.05829
-.06441
-.07052
-.07664
-.08276

Figure 18

29

FRINGE PLOT LC=2.2 RES=3.1(Y-COMP) MSC/PATRAN R-1.4 MSC/NASTRAN 18-Mar-96 13:24:48

DEFORMATION PLOT LC=2.2 RES=3.1 MSC/PATRAN R-1.4 MSC/NASTRAN 18-Mar-96 13:24:48

t1=.9375", 74.1 ksi, y-displacement

.004881
.003187
.001492
-.0002022
-.001897
-.003591
-.005286
-.006980
-.008675
-.01037
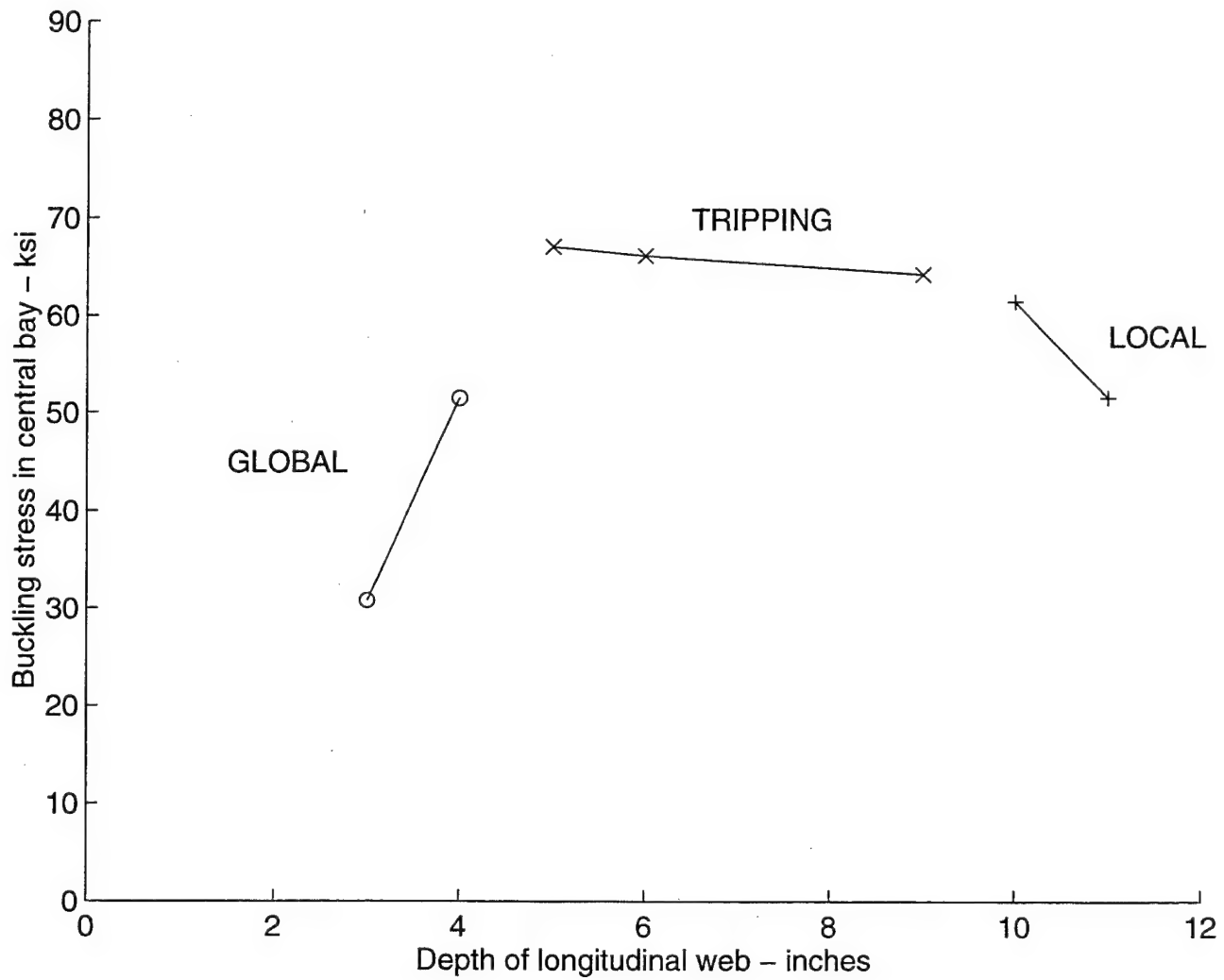-.01206
-.01376
-.01545
-.01715
-.01884
-.02054

Figure 19

Figure 20

FRINGE PLOT: LC=2.2 RES=3.1(VEC-MAG) MSC/PATRAN R-1.4 MSC/NASTRAN 01-Apr-96 10:33:06
DEFORMATION PLOT: LC=2.2 RES=3.1 MSC/PATRAN R-1.4 MSC/NASTRAN 01-Apr-96 10:33:06

dw1=4", 51.5 ksi, Magnitude of displacement

.1890
.1764
.1638
.1512
.1386
.1260
.1134
.1008
.08821
.07560
.06300
.05040
.03780
.02520
.01260
.00000004100

Figure 21

32

FRINGE PLOT, LC=2.2 RES=3.1 (VEC-MAG) MSC/PATRAN R.1.4 MSC/NASTRAN 01-Apr-96 10:53:46
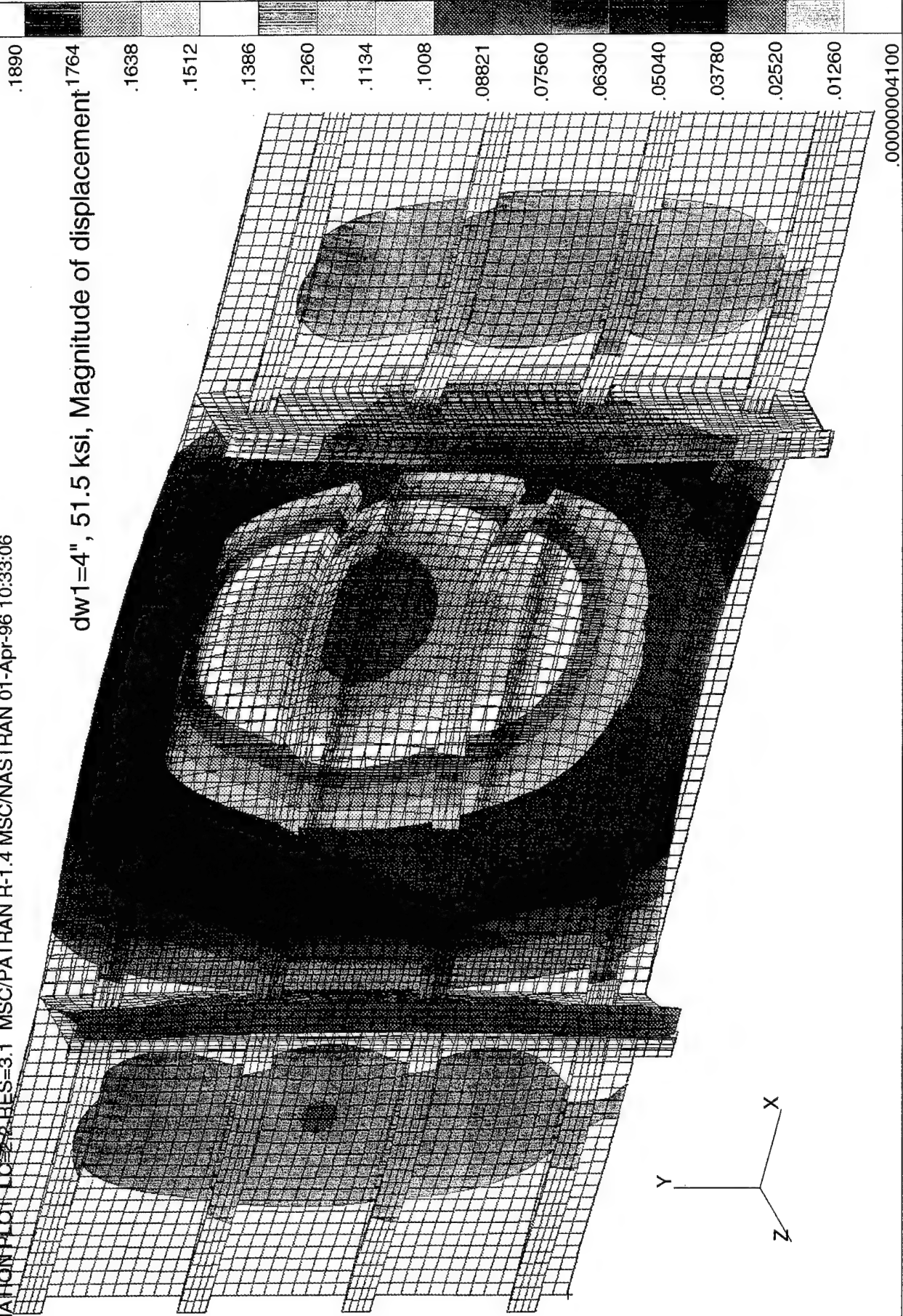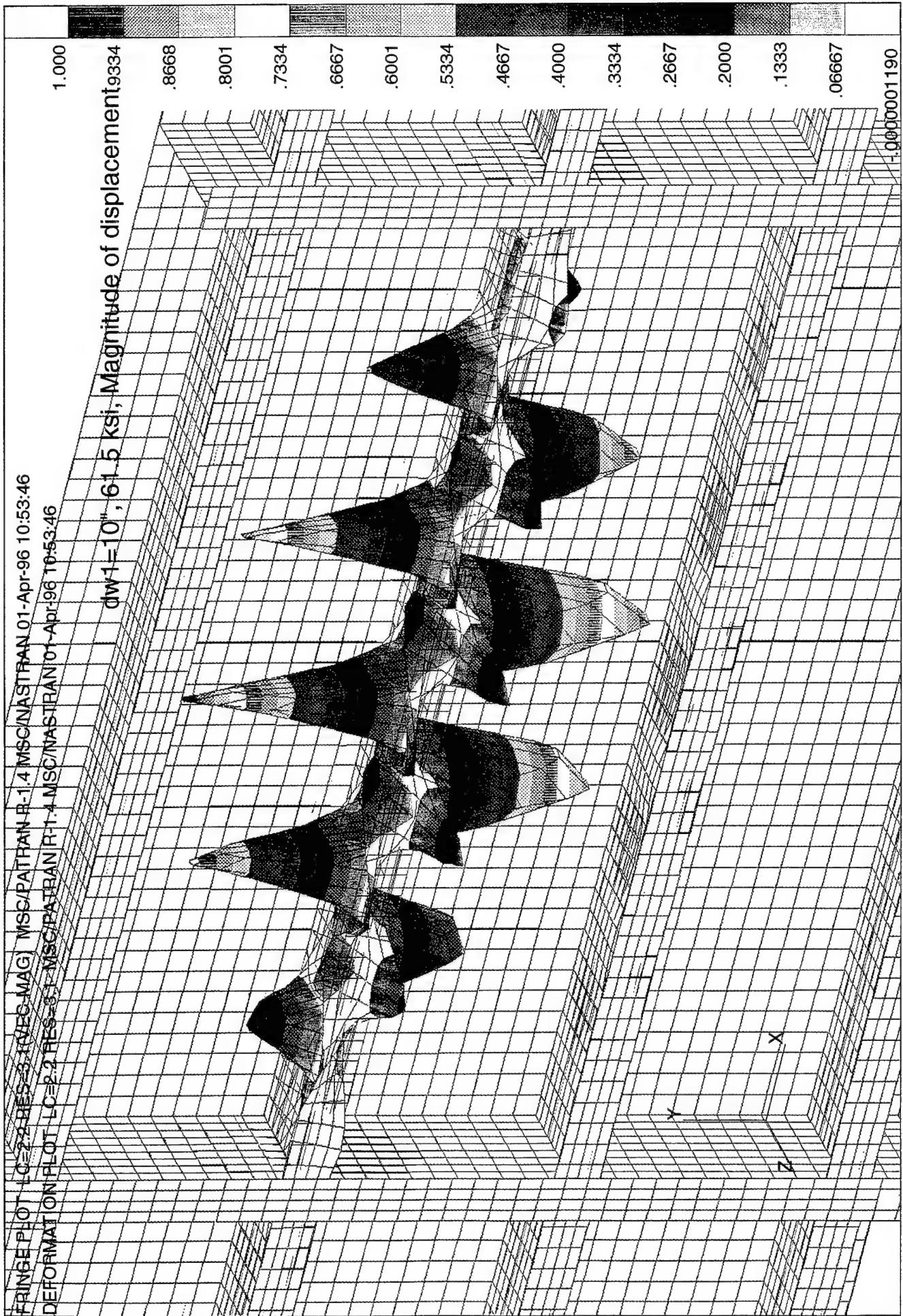DEFORMATION PLOT, LC=2.2 RES=3.1 MSC/PATRAN R-1.4 MSC/NASTRAN 01-Apr-96 10:53:46

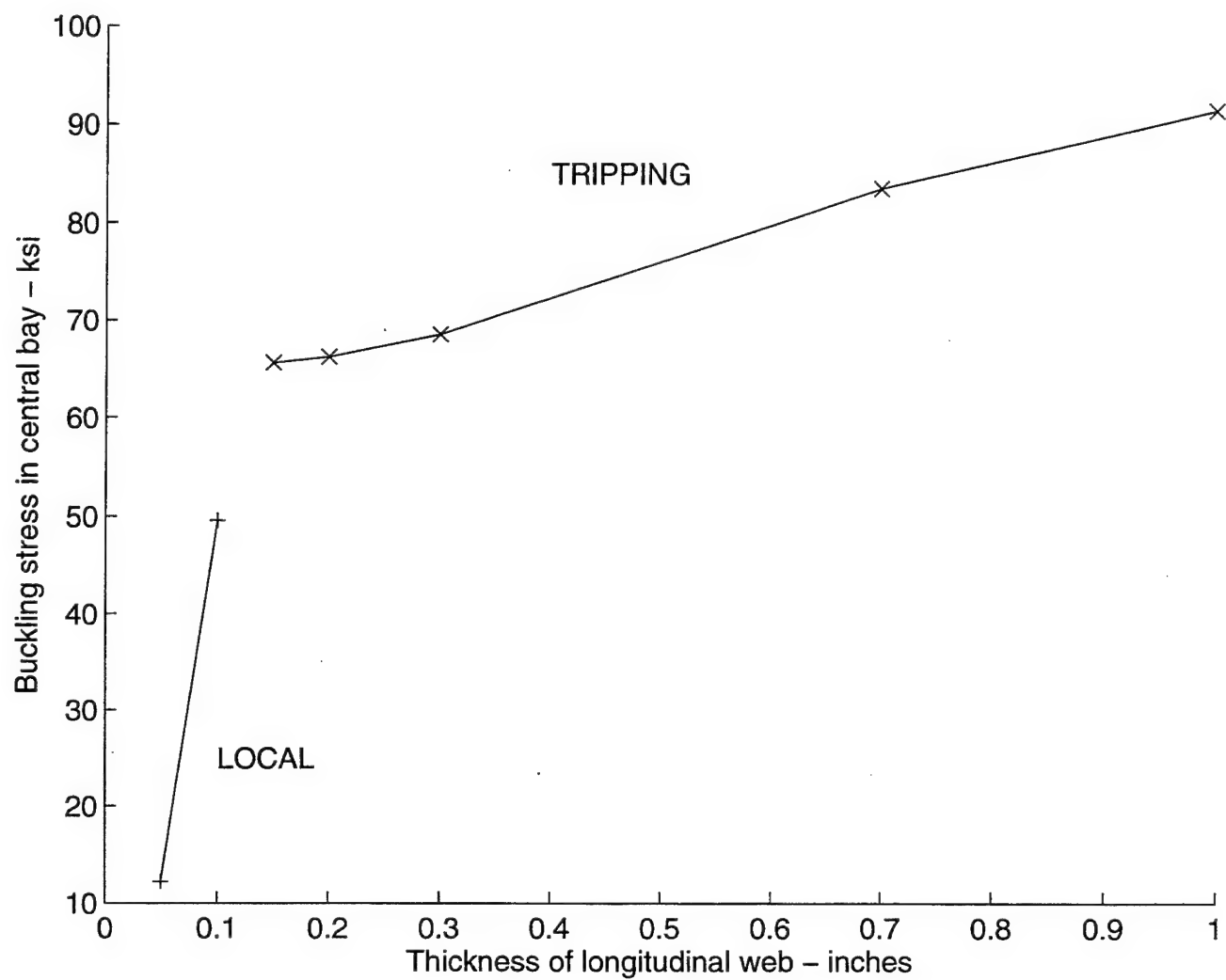dw1=10", 61.5 ksi, Magnitude of displacement

1.000
.9334
.8668
.8001
.7334
.6667
.6001
.5334
.4667
.4000
.3334
.2667
.2000
.1333
.06667
-.000001190

Figure 22

33

Figure 23

FRINGE PLOT: LC=2.2 RES=3.1(VEC-MAG) MSC/PATRAN R-5.0 MSC/NASTRAN 28-Jun-96 12:50:56
DEFORMATION PLOT: LC=2.2 RES=3.1 MSC/PATRAN R-5.0 MSC/NASTRAN 28-Jun-96 12:50:56
tw1=.1", 49.6 ksi, Magnitude of displacement

1.000
.9333
.8667
.8000
.7333
.6667
.6000
.5333
.4667
.4000
.3333
.2667
.2000
.1333
.06667
-.0000004500

Figure 24

35

FRINGE PLOT LC=2,3 RES=3.1(VEC-MAG) MSC/PATRAN R-5.0 MSC/NASTRAN 28-Jun-96 15:18:28
DEFORMATION PLOT LC=2,2 RES=3.1 MSC/PATRAN R-5.0 MSC/NASTRAN 28-Jun-96 15:18:28

tw1=.7", 83.5 ksi, Magnitude of displacement

1.000
.9334
.8668
.8001
.7334
.6667
.6001
.5334
.4667
.4000
.3334
.2667
.2000
.1333
.06667
.00000007500

Figure 25

36

Figure 26

FRINGE PLOT, LC=22 RES=3.1(VEC-MAG) MSC/PATRAN R-5.0 MSC/NASTRAN 02-Jul-96 12:28:02
DEFORMATION PLOT, LC=22 RES=3.1 MSC/PATRAN R-5.0 MSC/NASTRAN 02-Jul-96-12:28:02

df1=0, 30.8 ksi, Magnitude of displacement

1.001
.9343
.8675
.8008
.7341
.6673
.6006
.5339
.4671
.4004
.3337
.2669
.2002
.1335
.06673
-.0006001790

Figure 27

38

Figure 28

FRINGE PLOT: LC=2.2 RES=3.1(VEC-MAG) MSC/PATRAN R-5.0 MSC/NASTRAN 05-Jul-96 10:58:02
DEFORMATION PLOT: LC=2.2 RES=3: MSC/PATRAN R-5.0 MSC/NASTRAN 05-Jul-96 10:58:02

tf1=.1", 64.5 ksi, Magnitude of displacement

1.002	
.9354	
.8686	
.8018	
.7350	
.6682	
.6013	
.5345	
.4677	
.4009	
.3341	
.2673	
.2004	
.1336	
.06682	
.006000004500	

Figure 29

40

Figure 30

Figure 31

42

FRINGE PLOT LC=2.2 RES=3.1(VEC MAG), MSC/PATRAN R:50 MSC/PATRAN 10-Jul-96 14:16:31
DEFORMATION PLOT LC=2.2 RES=3.1 MSC/PATRAN R:5.0 MSC/PATRAN 10-Jul-96 14:16:31

tw2=-.1", -54.2 ksi, Magnitude of displacement

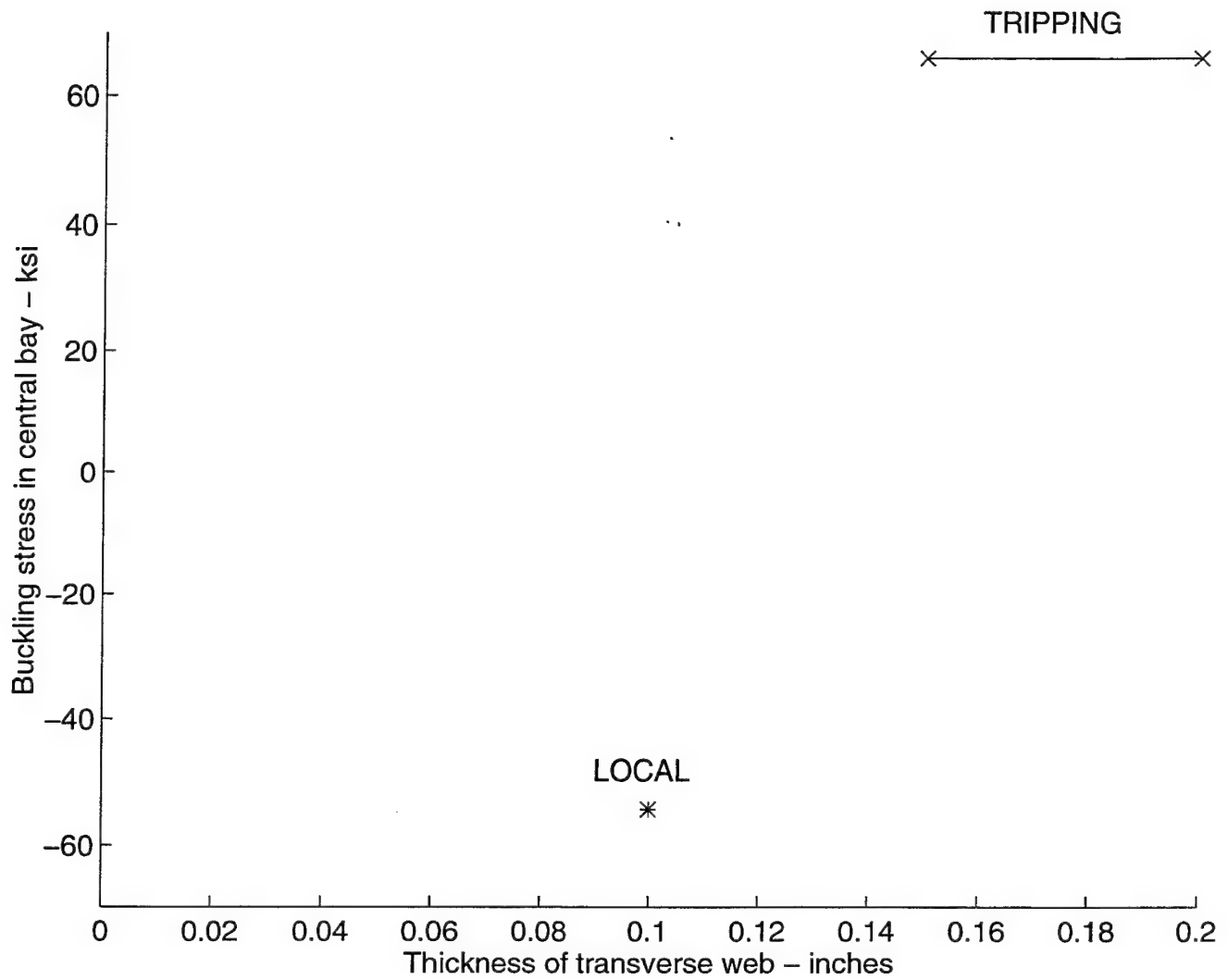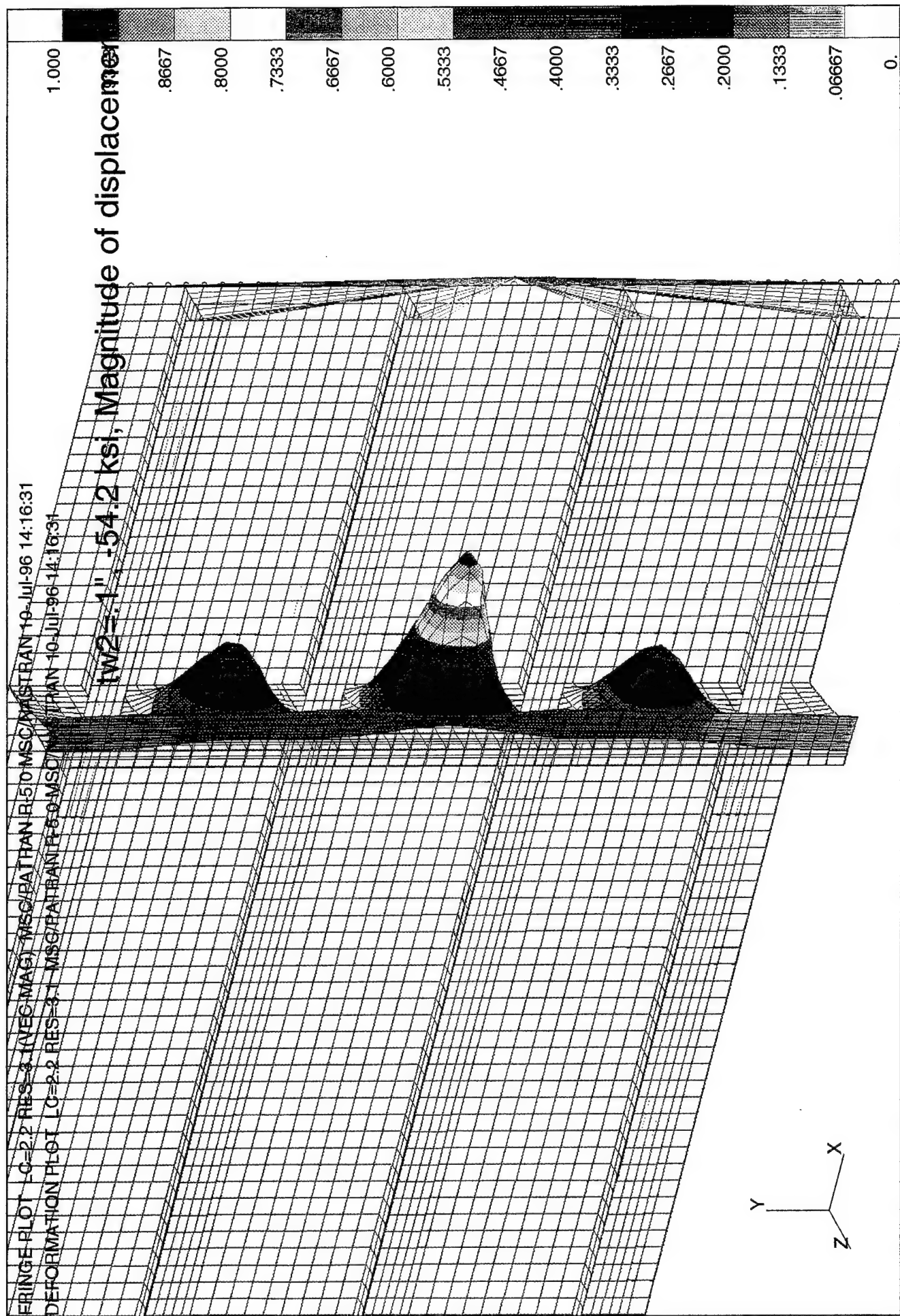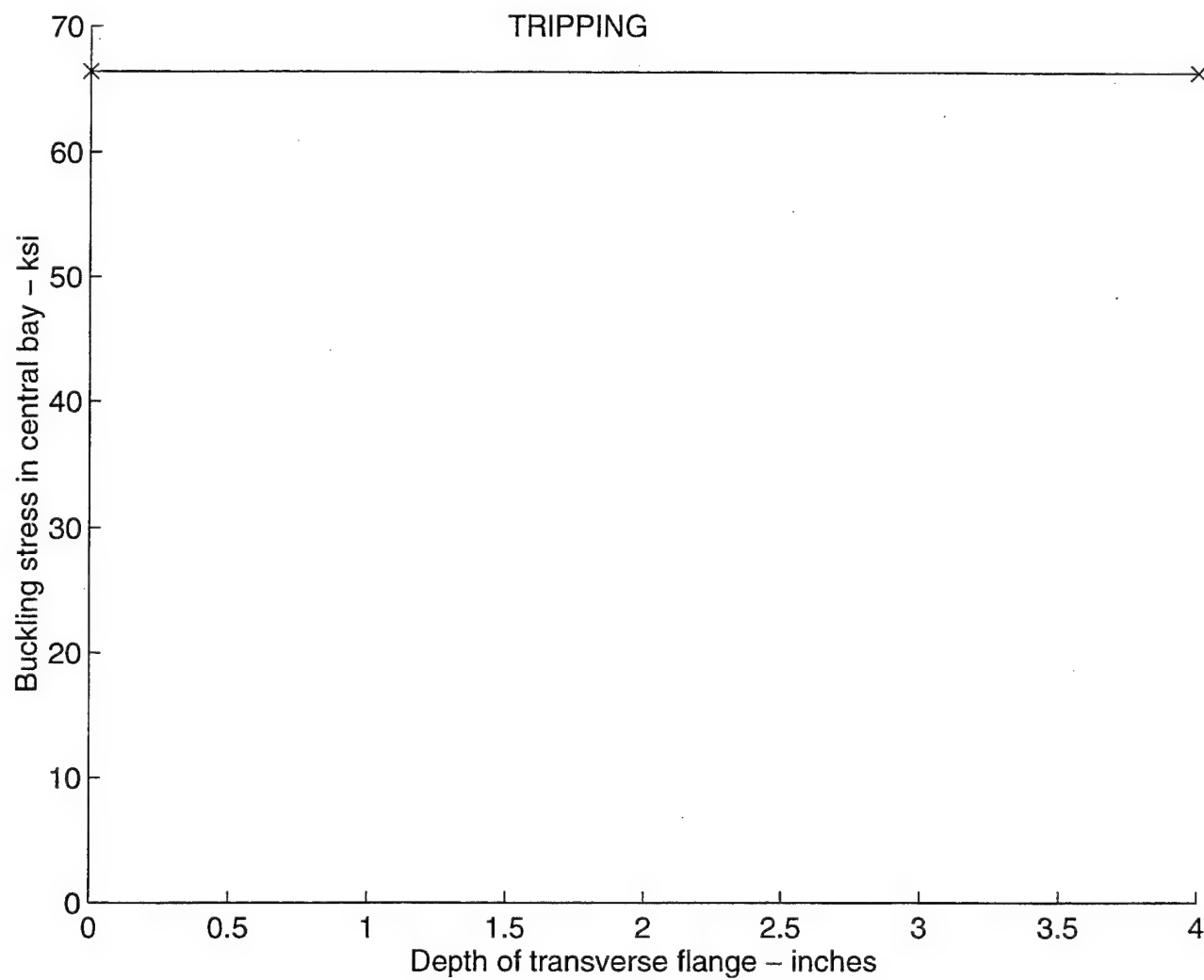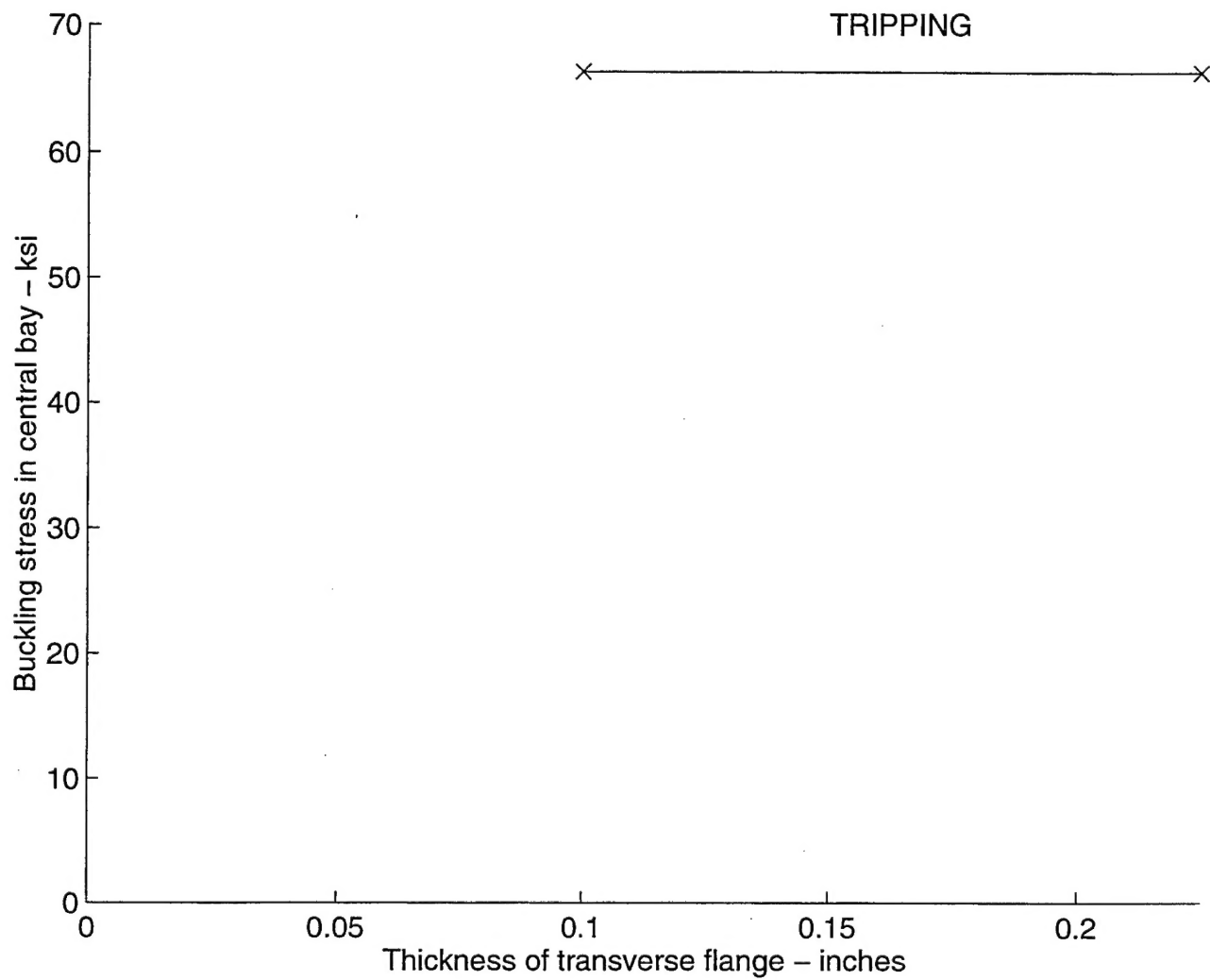|	
1.000	
.8667	
.8000	
.7333	
.6667	
.6000	
.5333	
.4667	
.4000	
.3333	
.2667	
.2000	
.1333	
.06667	
0.	

Figure 32

43

Figure 33

Figure 34

CONCLUSIONS

We can think of the buckling stress as being represented by a surface in n-dimensional parameter space (n = 11 in our studies). The surface is continuous but has discontinuous slope at the boundaries between subsurfaces corresponding to TRIPPING, GLOBAL, or LOCAL modes. Our curves of buckling stress versus a parameter are the intersections of the surface with vertical planes passing through a given point on the surface.

To fit the entire surface with an analytical approximation would appear to be a difficult computational problem requiring the calculation of numerous points on the surface. The parameter dependence of the buckling load is coupled, i.e., all the parameters would have to be varied simultaneously.

In future work the finite element eigenvalue code could be used to design the ideal structure. One possible design criterion would be to find the grillage of minimum weight among all possible grillages with buckling stress equal to the yield stress. The candidate points would lie on the intersection of the surface with a horizontal plane.

ACKNOWLEDGEMENTS

REFERENCES

Danielson, D. A., and Hodges, D. H. (1988). A beam theory for large global rotation, moderate local rotation, and small strain. *ASME Journal of Applied Mechanics* 55, 179-184.

Danielson, D. A., Kihl, D. P., and Hodges, D. H.(1990). Tripping of thin-walled plating stiffeners in axial compression. *Thin-Walled Structures* 10, 121-142.

Danielson, D. A., Cricelli, A. S., Frenzen, C. L. and Vasudevan, N. (1993). Buckling of stiffened plates under axial compression and lateral pressure. *International Journal of Solids and Structures* 30, 545-551.

Danielson, D. A.,(1994). Analytical tripping loads for stiffened plates. *International Journal of Solids and Structures.* 32, 1319 - 1328.

Danielson, D. A., Steele, C. R., Fakhroo, F. and Cricelli, A. S. (1994). Stresses in Ship Plating. *Naval Postgraduate School Technical Report* NPS-94-008.

Distribution List

	No. of copies
Director Defense Technology Information Center Cameron Station Alexandria, VA 22314	2
Director of Research Administration Code 81 Naval Postgraduate School Monterey, CA 93943	1
Library Code 52 Naval Postgraduate School Monterey, CA 93943	2
Chairman, Code MA Department of Mathematics Naval Postgraduate School Monterey, CA 93943	2
Professor D. A. Danielson Code MA/Dd Naval Postgraduate School Monterey, CA 93943	30
Dr. Marc Lipman Mathematical, Computer and Information Sciences Division Office of Naval Research 800 Quincy Street Arlington, VA 22217-5000	1
Dr. David Kihl Survivability, Structures, and Materials Directorate Naval Surface Warfare Center-Carderock Divison Bethesda, MD 20084-5000	5